Operational optimization of an industrial energy system considering balancing energy markets

by Stefan Haider BSc

A thesis for the degree of

Master of Science (MSc or Dipl.-Ing. or DI)

In the

Master program Mechanical Engineering

At the

Faculty of Mechanical Engineering and Management, TU Wien

Supervised by

Hofmann, Rene; Univ.Prof. Dipl.-Ing. Dr.techn.

Fischer, Martin; Projektass. Dipl.-Ing. BSc

Author
Stefan Haider BSc
Matr. Nr.: 01525486

Supervisor
Hofmann, Rene; Univ.Prof. Dipl.-Ing. Dr.techn. -habil
TU Wien
Institute for Energy Systems and Thermodynamics
Getreidemarkt 9, A-1060 Wien

Supervisor
Fischer, Martin; Projektass. Dipl.-Ing. BSc
TU Wien
Institute for Energy Systems and Thermodynamics
Getreidemarkt 9, A-1060 Wien

Affidavit

I declare in lieu of oath, that I wrote this thesis and performed the associated research myself, using only literature cited in this volume. If text passages from sources are used literally, they are marked as such. I confirm that this work is original and has not been submitted elsewhere for any examination, nor is it currently under consideration for a thesis elsewhere.

I acknowledge that the submitted work will be checked electronically-technically using suitable and state-of-the-art means (plagiarism detection software). On the one hand, this ensures that the submitted work adheres to the high-quality standards of the current rules for ensuring good scientific practice "Code of Conduct" at the Vienna University of Technology. On the other hand, a comparison with other students' theses avoids violations of my copyright.

Vienna, April 20, 2023

Stefan Haider

Abstract

The increasing share of volatile renewable energies in the European energy system is closely linked to new challenges for grid stability. Due to these upcoming changes in energy production, the design of the balancing energy market must also be adapted. The resulting flexibilisation of the balancing energy markets will create new economic fields, as participation will also be possible for smaller industrial energy plants, e.g. in production plants. By participating in the balancing energy markets, industrial energy plants will not only increase profits or reduce costs, but also contribute to grid stability.

The main task of this diploma thesis is to create a formulation to implement the balancing energy market into an operational optimization framework of an industrial energy system, under consideration of valid guidelines. This goal is achieved with the use mixed integer linear programming.

Data used to obtain results of the optimization is generated trough historical data and an electricity price forecast using an NARX neural network. The modelling is done for the automatic frequency restoration reserve, since this level of the balancing energy market is a combines rather high revenues, with relative moderate prequalification effort.

Stage one uses the predicted day ahead electricity price, historical data for the photovoltaic system and the different levels of acceptance probability, which are determined by the price, for the capacity tender of the balancing market, to calculate the ideal schedule of the industrial energy system. A further distinction is made between positive and negative balancing energy. Since every bid can either be accepted or neglected and the amount possible scenarios are calculated according to $2^{\text{amount of Bids}}$ for both positive and negative balancing energy. The used stochastic approach allocates each of these scenarios a certain probability, likelihood of occurrence, these value are multiplied withe the expected revenues of the corresponding scenario, by building the sum of all these products, the expected revenue for the negative and positive energy tender are calculated. Additionally the offered volume has to be covered by the free capacity of the industrial energy system.

Stage two uses the results of stage one, and optimises the schedule according to the real electricity prices and the information if the bids have been accepted, called up or not.

To answer the main topic, is it economic useful for the operator of an industrial energy system to take part of the balancing energy market, four different use cases were investigated. Use Case 1 and 2 are considered for reasons of reference and Use Case 3A and 3B to generate information about the implementation of the balancing energy market. For all of them the industrial energy system is the same. Use Case 1 a constant electricity price is obtained, with a surcharge by buying a and reduction by selling the electricity. In Use Case 2 the day ahead prediction of the neural net is used for optimisation and for the calculation of the expanses the real day ahead price are used. In Use Case 3A and 3B the balancing market is implemented and the optimisation is done according to stage one. They differ through the acceptance in stage two, for Use Case 3A no bids are accepted or called and for Use Case 3B all bids are accepted and called up, which represent the best and the worst case. Three different days are used to compare the different use cases.

Kurzfassung

Der steigende Anteil volatiler erneuerbarer Energien im europäischen Energiesystem ist eng mit neuen Herausforderungen für die Netzstabilität verbunden. Aufgrund dieser anstehenden Veränderungen in der Energieerzeugung muss auch das Design des Regelenergiemarktes angepasst werden. Die daraus resultierende Flexibilisierung der Regelenergiemärkte wird neue wirtschaftliche Felder schaffen, da die Teilnahme auch für kleinere industrielle Energieanlagen, z.B. in Produktionsbetrieben, möglich wird. Durch die Teilnahme an den Regelenergiemärkten können industrielle Energieanlagen nicht nur ihre Gewinne steigern oder ihre Kosten senken, sondern auch einen Beitrag zur Netzstabilität leisten.

Die Hauptaufgabe dieser Diplomarbeit ist es, eine Formulierung zur Implementierung des Regelenergiemarktes in einen betrieblichen Optimierungsrahmen eines industriellen Energiesystems, unter Berücksichtigung gültiger Richtlinien, zu erstellen. Dieses Ziel wird mit Hilfe der gemischt-ganzzahligen linearen Programmierung erreicht.

Die Daten, die zur Gewinnung der Optimierungsergebnisse verwendet werden, werden durch historische Daten und eine Strompreisprognose unter Verwendung eines neuronalen Netzes generiert. Die Modellierung erfolgt für die automatische Frequenzwiederherstellungsreserve, auch Sekundärregelenergie genannt, da es sich bei dieser Ebene des Regelenergiemarktes um eine Kombination aus verhältnismäßigen hohen Erlösen und mit einem moderaten Präqualifikationsaufwand handelt.

In der ersten Stufe wird anhand des prognostizierten Strompreises für den Folgetag, historischer Daten für die Photovoltaikanlage und der unterschiedlichen Preisniveaus, für den Leistungsausschreibung des Regelenergiemarktes der ideale Fahrplan des industriellen Energiesystems berechnet. Des weiteren wird zwischen positiver und negativer Regelenergie unterschieden. Da jedes Gebot entweder angenommen oder abgehlent werden kann ergibt sich die Anzahl der möglichen Szenarien nach der Gesetzmäßigkeit $2^{\text{Anzahl der Angebote}}$ sowohl für positive als auch für negative Regelenergie. Der verwendete stochastische Ansatz ordnet jedem dieser Szenarien eine bestimmte Eintrittswahrscheinlichkeit zu, diese Werte werden mit den erwarteten Erlösen des entsprechenden Szenarios multipliziert, durch Bildung der Summe

aller dieser Produkte werden die erwarteten Erlöse für die negative und positive Energieausschreibung berechnet. Zusätzlich muss die angebotene Menge durch die freie Kapazität des industriellen Energiesystems gedeckt werden.
Die zweite Stufe nutzt die Ergebnisse der ersten Stufe und optimiert den Fahrplan anhand der realen Strompreise und der Information, ob die Gebote angenommen, abgerufen oder nicht abgerufen wurden.
Zur Beantwortung der Hauptfrage, ob es für den Betreiber eines industriellen Energiesystems wirtschaftlich sinnvoll ist, am Regelenergiemarkt teilzunehmen, wurden vier verschiedene Anwendungsfälle untersucht. Die Anwendungsfälle 1 und 2 werden als Referenz betrachtet und die Anwendungsfälle 3A und 3B, um Informationen über die Implementierung des Regelenergiemarktes zu erhalten. In allen Fällen ist das industrielle Energiesystem identisch. Im Anwendungsfall 1 wird ein konstanter Strompreis erzielt, mit einem Aufschlag beim Kauf und einer Reduktion beim Verkauf des Stroms. In Anwendungsfall 2 wird die Vorhersage des neuronalen Netzes für den nächsten Tag zur Optimierung verwendet, und für die Berechnung der Kosten werden die realen Preise für den nächsten Tag verwendet. In den Anwendungsfällen 3A und 3B wird der Regelenergiemarkt implementiert und die Optimierung erfolgt entsprechend der ersten Stufe. Sie unterscheiden sich durch die Annahme in der zweiten Stufe, für Use Case 3A werden keine Gebote angenommen oder abgerufen und für Use Case 3B werden alle Gebote angenommen und abgerufen, was den besten und den schlechtesten Fall darstellt. Zum Vergleich der verschiedenen Anwendungsfälle werden drei verschiedene Tage herangezogen.

Acknowledgments

I am very grateful to my thesis advisor, Prof. Rene Hofmann, who gave me the chance to engage myself in this research activity. It was a great experience to be involved in this challenging state of the art topic.

I would like to thank all my colleagues at the Institute of Energy Systems and Thermodynamics, who always support me in the challenges ahead. I am particularly grateful for the supervision provided by Dipl.-Ing. Martin Fischer. He was my co-supervisor, who motivated me for the topic and generally supported me in this thesis.

Furthermore, I would also like to thank my colleagues who accompanied me during my studies, because our mutual support made all this possible.

Special thanks to Andrea Ungersböck BEd Ing, a professor at the HTL Hollabrunn, who encouraged me at the beginning of my technical education to continue even in difficult times, without her I would not be where I am today.

Finally, I would like to express my deepest gratitude to my parents, Anna and Josef, and my brother Michael for their constant support during my studies. Thank you for your constant encouragement and for your tireless patience.

Attitude is a little thing that makes a big difference.
-*Winston Churchill*

Danksagungen

Ich bin, Prof. Rene Hofmann, sehr dankbar, dass er mir die Möglichkeit gegeben hat, mich auf diesem Forschungsgebiet zu vertiefen. Es war eine großartige Erfahrung, an einem so akutellen und herausfordernden Thema, mitzuarbeiten zu dürfen.

Ich bedanke mich bei allen Kolleginnen und Kollegen des Instituts für Energietechnik und Thermodynamik, die mich stets unterstützt haben. Besonders dankbar bin ich für die Betreuung durch Dipl.-Ing. Martin Fischer, der mich als Co-Betreuer durch diese Arbeit geführt und das Thema allgemein vorangebracht hat.

Außerdem möchte ich mich bei meinen Kollegen bedanken, die mich während meines Studiums begleitet haben, denn nur unsere gegenseitige Unterstützung hat all dies ermöglicht.

Besonderer Dank gilt Andrea Ungersböck BEd Ing, einer Professorin an der HTL Hollabrunn, die mich zu Beginn meiner technischen Ausbildung ermutigt hat, auch in schwierigen Zeiten weiterzumachen, ohne sie wäre ich heute nicht da, wo ich bin.

Schließlich möchte ich meinen Eltern, Anna und Josef, und meinem Bruder Michael für ihre ständige Unterstützung während meines Studiums, meinen tiefsten Dank aussprechen. Vielen Dank für eure unermüdliche Geduld.

> Die Einstellung ist eine Kleinigkeit, die einen großen Unterschied macht.
>
> -*Winston Churchill*

Contents

Nomenclature

Acronyms

ACER Agency for the cooperation of Energy Regulators

aFRR automatic Frequency restoration reserve

APG Austrian Power Grid

BSP balancing service provider

DA day-ahead

DA-bid direct activated bid

ENTSO-e European network of transmission system operators - electricity

FCA forward power allocation

FCR frequency containment reserve

GCT gate closure time

GOT gate open time

ID intra-day

MARI Manually Activated Reserves Initiative

mFRR manual Frequency restoration reserve

MILP mixed integer linear programming

OTC over the counter

PCR primary control reserve

PICASSO Platform for the International Coordination of Automated Frequency Restoration and Stable System Operation

SA-bid scheduled activated bid

SDAC single day-ahead coupling

SIDC single intraday coupling

SRR secondary replacement reserve

TRR tertiary replacement reserve

TSO transmission system operator

Subscripts

0 initial value

C charge

CHP combined heat power plant

DA day-ahead

DC discharge

boiler boiler

cap capacity

ch change

coeff coefficient

EES electric energy storage

el electricity

energy energy

EVR expected value of revenues

f fuel

fG from Grid

in inactive

l liquid

LAP	level of acceptance probability
LoO	likelihood of occurrence
max	maximum value
mB	maximum bids
min	minimum value
neg	negative tender (capacity or energy)
peak	peak value
pred	predicted value
PV	photovoltaik
real	real value
rev	revenues
TES	thermal energy storage
tG	to Grid
therm	thermal
VE	value expected

Variables and Parameters

A	general parameter	-
B	bid related parameter	-
C	capacity	$\mathrm{MW\,h}$
F	flow	$\mathrm{MW\,h\,h^{-1}}$
H	energy	$\mathrm{kW\,kg^{-1}}$
L	load	$\mathrm{MW\,h}$
P	power	MW
PS	possible scenarios	-

F	scenarios	-
F	time	h
c	costs	€
m	massflow	$\mathrm{kg\,h^{-1}}$
r	revenues	€
η	efficiency	-

List of Figures

List of Tables

1 Introduction

1.1 Motivation

On May the 18th of 2022 the EU Commission presented the REPowerEU-plan, it's main target is to raise the amount of renewable energy in the European Union up to 45 % until 2030. This will help address the climate crisis and also reduce the dependence on fossil fuels. Figure 1 shows the annual change of net installed electricity generation capacity in Europe in 2022. As can be seen there, the share of renewable energy sources has increased buy up to 40 GW.

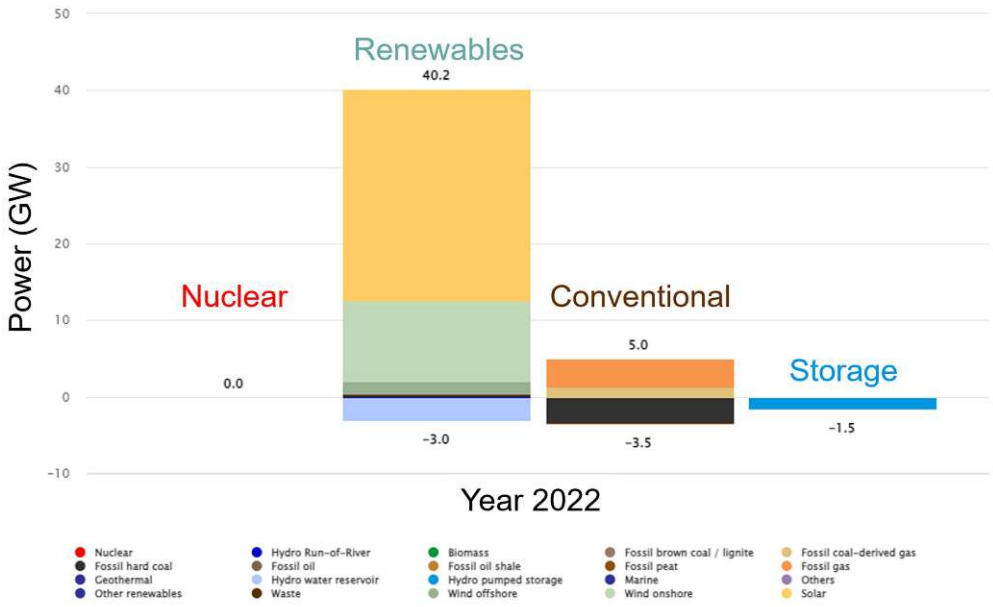

Figure 1: *Annual change of net installed electricity generation capacity in Europe in 2022 [1]*

1.2 Problem statement

Due to the rising amount of volatile renewable energy sources, the European energy grid, known as the biggest machinery built by mankind, faces big challenges. In the case of Austria, this can be seen by the amount of money spent from Autrian Power Grid (APG) for both the balancing energy as well as for re-dispatches. Balancing energy is needed to ensure a constant frequency level in the energy grid, while re-dispatches are needed to avoid an overload of parts of the energy grid.
Due to the change in energy supply, the system of balancing energy and redispatches must also be adapted. For the balancing energy market one novelty are reduced bidding periods, which should increase the number of market participants.

1.3 Aim of this thesis

The flexibilisation of the balancing energy markets will create new economic fields, as participation will also be possible for smaller industrial energy plants, e.g. in production plants. By participating in the balancing energy markets, industrial energy plants will not only increase profits or reduce costs, but also contribute to grid stability. In order to be able to make decisions in these newly created market-based fields, new methods are needed, which were developed in the context of this thesis. Since the balancing energy market is difficult to predict, a stochastic approach is used here in combination with classical operational optimisation. The implemented MATLAB® optimisation should offer high usability in regards to running and evaluating the ideal schedule for the given industrial energy system, additionally parameters describing the industrial energy system should be easy changeable in a convenient way.

1.4 Methodological approach

The stated problem was analysed with regard on the given energy market design as well as the changes announced. To this end, a thorough study of relevant academic literature was undertaken.

To be able to achieve the ideal schedule of the industrial energy system mathematical optimization has been chosen. Since the balancing energy market is subject to uncertainties in both pricing and acceptance a stochastic approach is implemented

to the linear optimisation problem. All possible scenarios that may appear are connected to a level of likelihood, which will allows to generate the most likely result of the balancing market. To be able to perform this optimisation, open source date, for e.g. price levels, called up energy is used.

After this short introduction into the thematic of the problem, this diploma thesis is structured as follows.

In Chapter 2, the theoretical framework of electricity market design for Europe and Austria is given. This summary, based on literature review, should provide the reader of this thesis with the most essential knowledge to comprehend the documentation in the subsequent chapters

In Chapter 3, the fundamental considerations for the further thesis are described, as well as the used model structure for the implementation in MATLAB®. This is followed by the data analysis, where the source of the used data is given with the additional pre-processing which is needed for the optimisation. The implementation of the given industrial energy system as well as the additions needed for the balancing energy are also in this chapter.

In Chapter 4 the different models used for the verification of this optimisation are explained, compared and discussed. Therefore the way, how the electric and thermal demand are met are visualised and the expenses and revenues of different days are compared for each model.

Chapter 5 closes this thesis with assertions gained during its production and their discussion. Finally, improvements and future research objectives are suggested.

2 Electricity Market Design

This chapter deals with the Austrian and the European electricity market design and its future prospects. It is built on three pillars as seen in the following Figure 2. The first of them is, the so called Energy-Only-Market, where electricity for industry and households is traded for long and short term. The second one are system services. One part of this pillar is the so called balancing energy which is indispensable to keep generation and consumption at an equal level. Due to the last pillar, transmission system operators (TSOs) or Federal Network Agencies are also able to intervene in the market, for reasons of grid stability. In Austria, the second and the third pillar are covered by the Austrian Power Grid (APG). Since the 1990 when the electricity and natural gas markets were monopolies five liberalisation directives, also called energy packages have been adopted and four, of them have been transposed into the member states legal system. The first liberalisation directive (adopted in 1996 for electricity and for natural gas in 1998 and transposed for electricity in 1998 and for natural gas in 2000) aimed to open the electricity and natural gas markets gradually to competition. With the second liberalisation directive (adopted in 2003 and transposed in between 2004 - 2007) industrial and domestic consumers were free to choose their own supplier for natural gas and electricity. In the third liberalisation directive (in 2009) further liberalize the internal electricity and gas markets was adopted providing the cornerstone for the implementation of the internal energy market. The Fourth Energy package introduced new electricity market rules for renewable energies and for attracting investments. It consisting of one directive (Electricity Directive 2019/944/EU) and three regulations (Electricity Regulation 2019/943/EU, Risk-Preparedness Regulation 2019/941/EU and EU Agency for the Cooperation of Energy Regulators (ACER) Regulation 2019/942/EU). It required Member States to prepare contingency plans for potential electricity crises and increased ACER's competences for cross-border regulatory cooperation in cases involving risk of national and regional fragmentation. The fifth liberalisation directive targets with the new European climate ambitions for 2030 and 2050. The debate on its energy aspects is ongoing [2]. The European-Council confirmed the target of at

least 40% of the share of energy from renewable sources in 2030 in the Union's gross final consumption [3]. The liberalisation and the increasing share on volatile power generation will lead to big challenges in the balancing market. In order to deal with these challenges the European-Commission adopted in 2017 the Regulation (EU) 2017/2195, which established a guideline on electricity balancing.

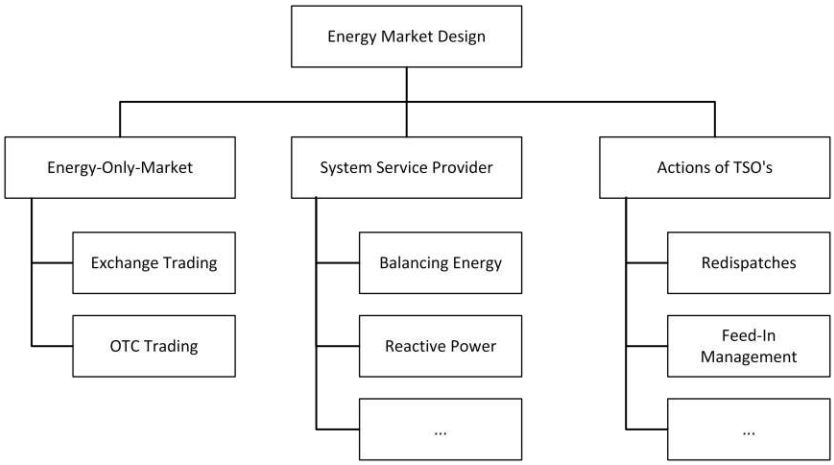

Figure 2: *Structure of the Energy Market Design.*

2.1 Price forming mechanisms

In the energy sector there are two different price forming mechanisms, on the one hand pay-as-cleared also known as uniform pricing and on the other hand pay-as-bid. In this section both of them are explained [4].

2.1.1 Pay-as-cleared

For the pay-as-cleared mechanism all supplies and demands have to be known. On the supply side, the order of the offers is determined due to increasing variable costs of each generation unit, this is also known as the merit order. The cheapest generation unit is therefore called first, followed by more expensive generation units, until market equilibrium is reached. This is shown in Figure 3. All called generation units are remunerated with the most expensive called generation unit.

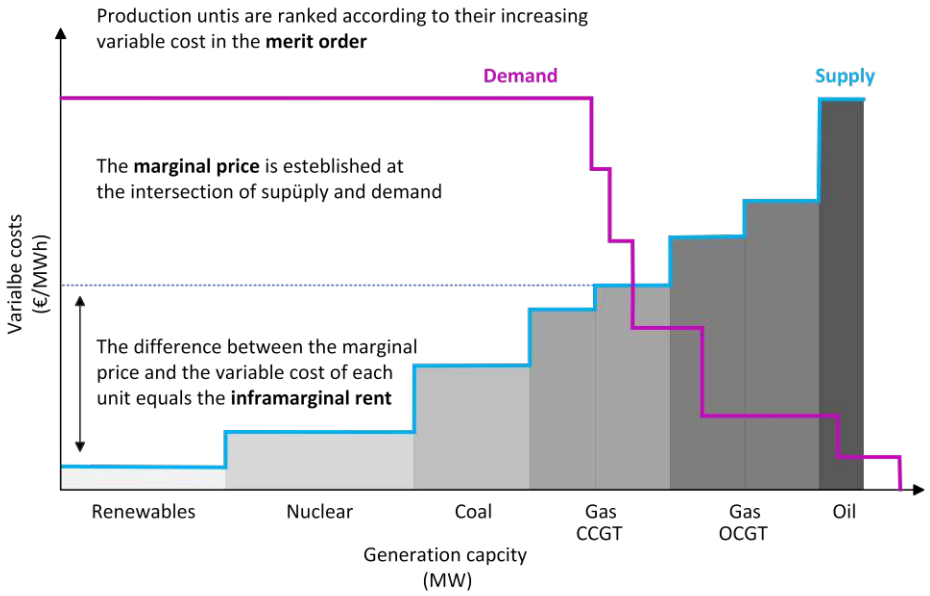

Figure 3: *Visualised pay-as-cleared mechanism [4].*

2.1.2 Pay-as-bid

At pay-as-bid the name says it all, every participant receive the price of their bid/offer. Therefore the electricity price depends no longer on the most expensive called generation unit, but on the average of all called units [4].

2.2 Energy Only Market

There are two ways in which energy can be traded. Either via exchange markets or through over the counter (OTC, bilateral) markets. While exchange trading takes place under special conditions, e.g. electricity price-dependent hedging, over-the-counter trading is very little restricted. Both trading opportunities are distinguished in long-term market and short-term or spot-market. This is shown in Figure 4.
The long-term market (annual and monthly products) is primarily used to hedge market participants transactions against the volatility of short-term trading and is governed by the provisions of the Forward power Allocation (FCA) Regulation (EU) 2016/1719.
The spot or short term market is divided in the so called Day-Ahead (DA) and Intra-Day (ID) trading. DA trading has many different tender types, with one-hour

orders being the most common. The gate closure time (GCT) depends on the used trading platform but is usually at 12:00 AM. At continuous ID trading gate opening time (GOT) depends also on the trading platform but usually starts one day before delivery (D-1) and closes up to 5 minutes (T-5) before delivery. At the ID markets 15, 30 as well as 60 minutes products are offered, depending on the country. In Austria there are only 15 minute products available.
In order to increase the overall efficiency of trading and to achieve a more efficient use of generation resources across Europe for DA and ID, the so-called European Network of Transmission System Operators for Electricity (ENTSO-e) has introduced Single Day-ahead Coupling (SDAC) as well as Single Intraday Coupling (SIDC) .
SDAC allocates scarce cross-border transmission power in the most efficient way by coupling wholesale electricity markets from different regions through a common algorithm, simultaneously taking into account cross-border transmission constraints thereby maximising social welfare [5]. SIDC works as followed, when a market participant submits an order for a different market area, it can be matched as long as there is enough transmission power available. To match an order simply means that the market participant can meet and supply the energy demand. Trading is done on a first-come-first-served principle where the highest buy price and the lowest sell price get served first [6].

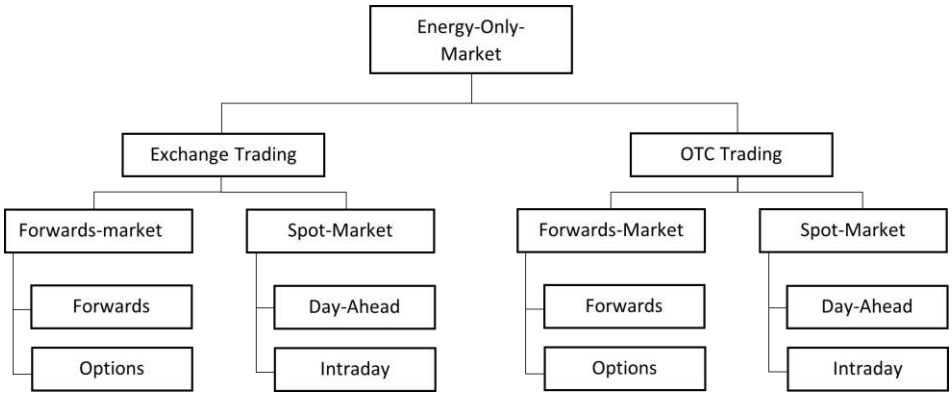

Figure 4: *Structure of the Energy Only Market Design.*

2.3 Balancing market

Electricity generation and electricity consumption must be exactly in balance at all times. The task of APG as the control area manager is to maintain this sensitive balance in Austria. The indicator for the quality of this balance and thus for

the supply quality of the end consumers is the grid frequency. It must always be approximately 50 Hz. If there is an imbalance between generation and consumption, the grid frequency fluctuates. If, for example, a large power plant fails, i.e. there is suddenly too little generation on the grid, the frequency drops. Conversely, the frequency rises above 50 Hz when less electricity is consumed than is generated. Due to the addition of highly fluctuating electricity generation from wind and solar power, APG has to intervene more frequently and with increasing effort to balance the grid [7]. In normal operation, the frequency should deviate from this setpoint by a maximum of 200 mHz [8]. Therefore the balancing market in Austria and in most parts of Europe is divided into three levels. The Frequency Containment Reserve (FCR) is a solidarity safety reserve geographically distributed over the synchronous area for the initial stabilisation of the frequency. It is needed to automatically compensate for a sudden imbalance between generation and consumption within a few seconds through appropriate activation (regulation). This prevents a continued increase in the frequency deviation - and subsequently a blackout. The Frequency Containment Reserve, which is distributed on the basis of solidarity, initially stabilises the frequency, but ultimately the control area in which the imbalance occurred is responsible for balancing it. The automatic frequency restoration reserves is an individual, automatically acting reserve that each control area must keep ready for itself. If an imbalance occurs in a control area, the secondary control reserve is activated in this control area (and only there). In this way, the common primary control reserve of continental Europe is relieved again and can fulfil its function as a safety net again. The manual frequency restoration reserves is also an individual reserve, is activated manually and supports or relieves the secondary control reserve if required. Basically, it serves to avoid a prolonged activation of the secondary control reserve (several quarter hours in a row), as it would then no longer be available for possible further deviations from equilibrium. The distinction between these three levels of balancing energy is made for technical and economic reasons, their activation area is shown in Figure 5, activation and utilisation time, is seen in Figure 6 as well as in their available capacities. Another difference is the so called prequalification, which is needed to take part of the different tenders. A distinction is made between power and energy tenders. Power tendering ensures that the required power is offered for the relevant day. It ends on the day before delivery. All balancing service providers (BSP) who have been accepted in the power tender must also participate in the energy tender. Here the actually required energy is tendered. BSPs get paid for power as well as for their actual delivered energy. As

(a) *FCR* (b) *aFRR* (c) *mFRR*

Figure 5: *Activation area of the different balancing energy levels.*

mentioned above, a BSP must be prequalified to participate in the various tenders. To obtain prequalification, the BSP must provide APG with a range of information on the grid connection, technical realisation, parameters of the system, function control, contact data, data transmission concept, form of transmitted data, balance group and grid operator. Prequalification of the three different balancing levels differs mainly in function control. Divergences are explained in the corresponding subsections.
Additionally an excerpt of the definition of terms from the commission regulation (EU) 2017/2195 "establishing a guideline on electricity balancing" is given.

- 'balancing market' means the entirety of institutional, commercial and operational arrangements that establish market-based management of balancing;
- 'balancing services' means balancing energy or balancing capacity, or both;
- 'balancing energy' means energy used by TSOs to perform balancing and provided by a balancing service provider;
- 'balancing capacity' means a volume of reserve capacity that a balancing service provider has agreed to hold and in respect to which the balancing service provider has agreed to submit bids for a corresponding volume of balancing energy to the TSO for the duration of the contract;
- 'balancing service provider' means a market participant with reserve-providing units or reserve-providing groups able to provide balancing services to TSOs;

2.3.1 Frequency Containment Reserves

The first stage of regulation is called Frequency Containment Reserve (FCR) or primary control reserve (PCR), it covers the entire European electricity grid and

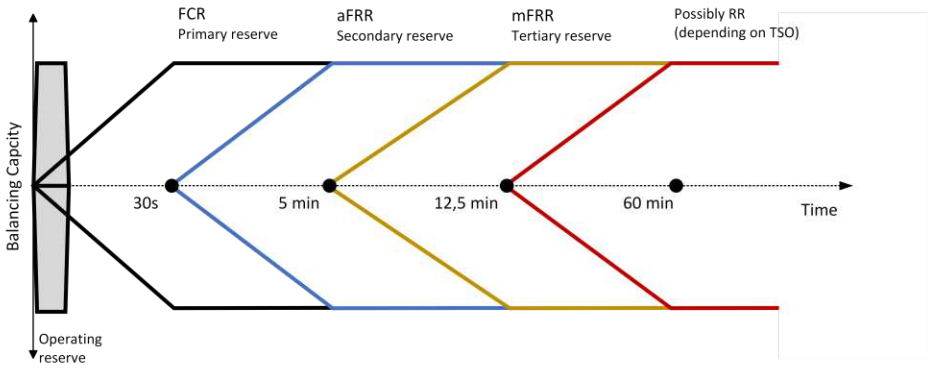

Figure 6: *Balancing Energy activation chart.*

is characterised by extremely short activation times (<30 seconds) and acts for a maximum of five minutes. The delivered energy averaged over time results in zero, therefore there is only a power tender. A day is divided into six four-hour blocks, an offer always refers to one of these blocks and must be at least 1 MW and may not exceed 25 MW in the case of indivisible offers, as seen in Table 1. In the FCR

Table 1: *Frequency Containment Reserves product parameters.*

tender	duration h	volume MW	min. offer MW	step size MW	max. offer MW	remuneration type
negative/ positive power	4	±73	±1	±1	±25	pay-as-cleared

power tender, there is no subdivision between positive and negative control power, which means that the offer must cover both cases. The total volume provided for Austria is ±73 MW and for the Europe ±3000 MW. Gate open time is 14 days before delivery at 11:00 AM and gate closure time is one day before at 8:00 AM, visualised in Figure 7. Each accepted bid is paid the price per MW corresponding to the highest accepted bid, also known as pay-as-cleared [9]. FCR is the highest paid level, but it also has the highest requirements for prequalification. Function control for FCR includes according to [9],

- accuracy of frequency measurement: The error in the frequency measurement of FCR must not exceed ±5 mHz.
- insensitivity range: For each technical unit, alias plant, an insensitivity range

of ±10 mHz is prescribed, in this range no FCR should be activated

- activation rate: At a frequency deviation of ±100 mHz, the 50 % of FCR must be activated after 15 seconds. If the frequency deviation is greater than $\pm 100 mHz$ the reserve has to be activated linearly so that the total reserve is fully activated after 30 seconds. For non-rotating units (discretely switchable), one-twentieth of the total reserve must be activated for each frequency deviation of ±10 mHz.
- reserve activation: The contracted reserve must be activated by the applicant; an application to APG is not required.
- reserve activation By frequency deviation > ±200 mHz: If technical possible a additional activation should not be limited.
- labour availability: At continuous activation the total reserve has to be provide for at least 30 minutes, at a frequency deviation of ±200 mHz. If the deviation is lower, the time period expenses.
- statics: For rotating technical units the adjustable range of statics has to be provided in the technical realisation. At non rotating technical units the equivalent characteristic curve has to be provided.

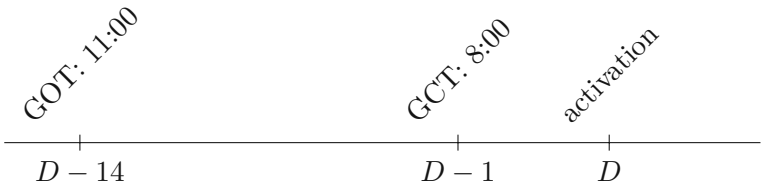

Figure 7: *Power tender-timeline for replacement reserves.*

2.3.2 Automatic frequency restoration reserves

The second level of balancing is called automatic frequency restoration reserves (aFRR) or secondary replacement reserve (SRR), which is intended to replace primary regulation in the event of a prolonged power fluctuation, so that primary regulation is again available for other unpredictable events. The duration of action are 15 minutes. In contrast to primary regulation, aFRR has to be covered by each transmission system operator himself, in Austria by APG. The aFRR power tender,

as in the primary regulation tender, the day is divided into six four-hour blocks, with a total volume of ±200 MW each. One of the differences is that positive and negative regulation reserve are tendered separately. Bid sizes are the same as for the primary power tender, as seen in Table 2. GOT is seven days before delivery at 10:00 AM and GCT is the day before delivery at 09:00 AM. Another difference to the tendering procedure of the primary regulation is the settlement methodology, here Pay as Bid is used, i.e. each BSP is paid the price included in its bid, provided that its bid is accepted, as shown in Figure 9 [10] .

APG is part of the project, Platform for the International Coordination of Automated Frequency Restoration and Stable System Operation or short PICASSO by ENTSO-e. PICASSO intends to reduce costs of aFFRs for participating TSOs by increasing flexibility trough shortened time slots and a so called cross boarder marginal pricing. The prerequisites for PICASSO have already been implemented in the energy tender; on the one hand, these enable trading across the borders of the TSO, and on the other hand, the blocks have been shortened to 15 minutes in order to achieve greater flexibility. This is intended to take better account of volatile renewable energy generation plants in particular, and also to enable more BSPs to participate in the market. The minimum bid quantity is 1 MW, with a maximum of 25 MW to be offered for indivisible bids. As with the power tender, a distinction is made between positive and negative energy tenders, also seen in Table 2. GOT is at 09:30 the previous day, GCT is 25 minutes before delivery (start of product). The results of this tender are published 25 minutes before a needed activation, as visualised in the timeline in Figure 8.

When PICASSO is fully implemented, cross-border marginal pricing is introduced as calculation for the remuneration. Here, an optimisation function calculates the marginal price for activation in each zone (TSO zones); if there is no bottleneck between two zones, the same marginal price is calculated. Since 2014 a lot of different models as well as shorter auctions have been tested. [11]

With the introduction of the new balancing market in 2020, the intervals of auctions have been reduced from daily to 4 hour tact. This has lead to a price reduction of more than 80 % from 2014 (203 mio €) to 2020 (40 mio €) [12] .

The functional control for aFRR according to [10] consists of

- Reaching the set point value: The applicant must activate the required secondary replacement reserve immediately upon APGs request. A time delay in the seconds range (reaction time) is permitted. Additionally a shortfall of 3 % is allowed as well as an overshoot of 10 %.

- Dynamic Control: A power gradient must be specified and demonstrated for each technical unit. After five minutes the maximum secondary replacement reserve has to be activated.

Table 2: *Automatic frequency restoration reserves product parameters.*

tender	duration h	volume MW	min. offer MW	step size MW	max. offer MW	remuneration type
positive power	4	+200	+1	+1	+25	pay-as-bid
negative power	4	−200	−1	−1	−25	pay-as-bid
positive energy	0.25	-	+1	+1	+25	pay-as-cleared
negative energy	0.25	-	−1	−1	−25	pay-as-cleared

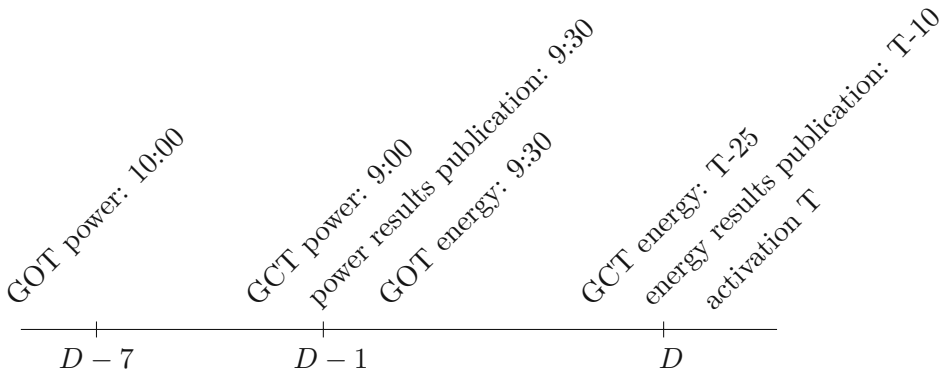

Figure 8: *Power and energy tender-timeline for automatic frequency restoration reserves.*

2.3.3 Manual frequency restoration reserves

Manual frequency restoration reserves (mFRR) describes the third level in the balancing market; it is activated manually or automatically when interruption duration last longer than the allowed time window from aFRR, it is also known as tertiary regulation reserve (TRR). Similar to aFRR, there is a project by ENTSO-e to make the market more flexible named Manually Activated Reserves Initiative (MARI). APG is also part of this project. Unlike PICASSO, MARI will go live in

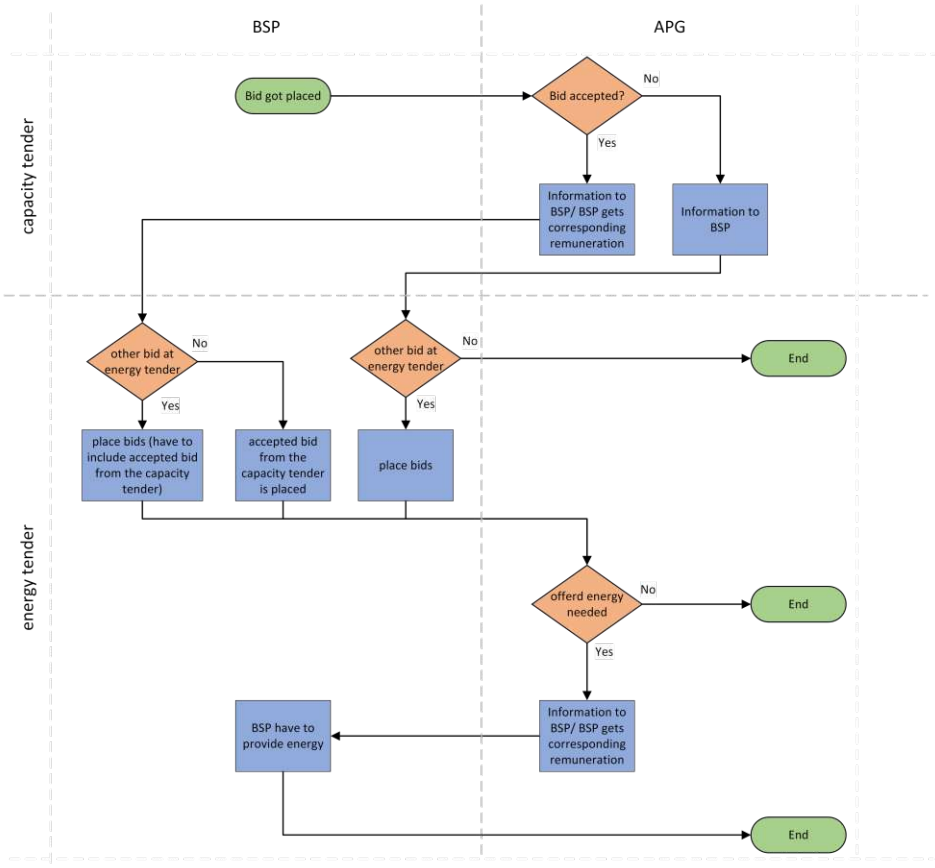

Figure 9: *Flow-diagramm of capacity and power tender form the aFRR and mFRR.*

the end Q2 of 2023 in Austria, that is why it has not yet been implemented in the electricity market design.

The tendering procedure for the mFRR is very similar to that of aFRR. The only differences are, GOT is seven days before delivery at 10:00 AM, GCT is one day before delivery at 10:00 AM and the total volume is at −195 MW and +280 MW. All Information about mFRR are summarised in Table 3 as well as in Figure 10.

Like the power tender, the energy tender is made up of six four-hour blocks. Positive and negative balancing energy are also tendered separately. The minimum bid is 10 MW, although this is also capped at 25 MW for indivisible bids. GOT is after 10:00 AM and GCT is always 60 minutes before delivery, the results of this tender are presented 30 minutes before activation [13].

The functional control for mFRR is similar to aFRR, but the maximum activation time of the dynamic control is up to ten minutes as in [13] explained. The

Table 3: *Manual frequency restoration reserves product parameters.*

tender	duration h	volume MW	min. offer MW	step size MW	max. offer MW	remuneration type
positive power	4	+280	+1	+1	+25	pay-as-bid
negative power	4	−195	−1	−1	−25	pay-as-bid
positive energy	4	-	+1	+1	+25	pay-as-bid
negative energy	4	-	−1	−1	−25	pay-as-bid

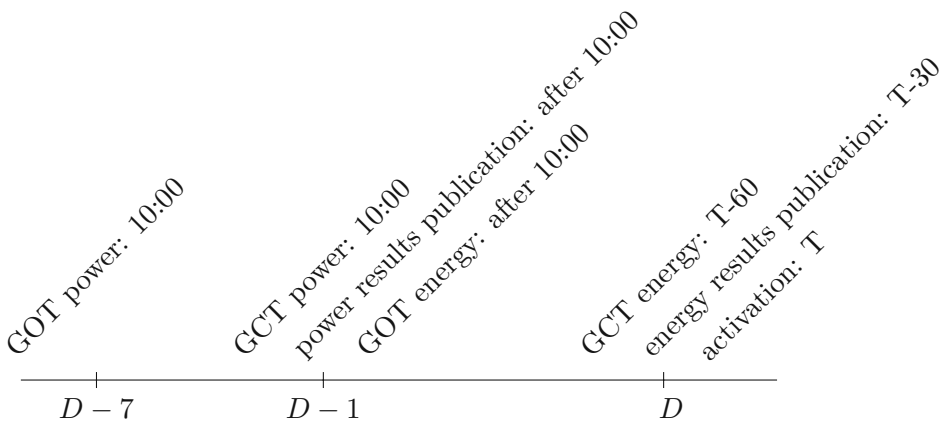

Figure 10: *Power and energy tender-timeline for manual frequency restoration reserves.*

introduction of MARI mainly changes the energy tendering of the mFRR. Blocks are shortened from four hours to quarter-hour blocks, and cross-border marginal pricing is introduced as in PICASSO. In addition, bids are submitted either as scheduled activation (SA bid) or as scheduled and direct activation (DA bid). SA bids can only be activated every quarter of an hour and DA bids can be called at any time. This leads also to changes in the tender-timeline. For MARI there are two different GCT used, one for BSPs and the second one for TSOs [14].

For scheduled activation BSP GCT is T-25, then the TSOs compute their demand and have to submit all bids and demands to the MARI platform. The market clearing is completed after 60 seconds. At T-7.5 the BSP will receive the clearing information and must ramp up or down according to the activation in 12.5 minutes.

So the full power exchange will take place between T+5 and T+10, visualised in Figure 11. After the scheduled activation are completed, direct activations take

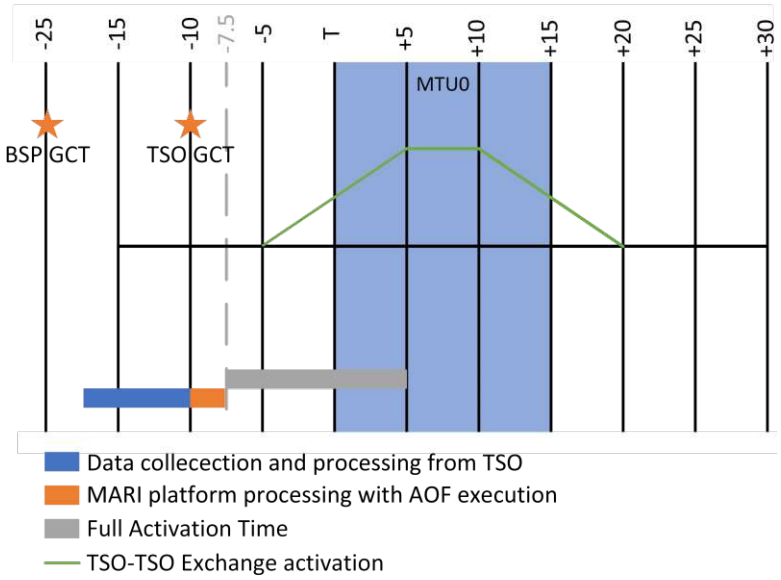

Figure 11: *Scheduled activation in MARI [14].*

place. Only reaming bids available for DA in the same direction as the demands are considered here. After T-10 any TSO is able to report a demand for DA, the MARI platform needs 15 seconds to perform clearing. Between T-7.5 and T+7.5 the BSP is informed. This scheme is shown in Figure 12.

2.3.4 Balancing energy from industrial energy systems

Due to the introduction from PICASSO and MARI time-slots for the energy tender at aFRR and mFRR are reduced from 4 hours to 15 minutes. This Fact will lead to both, more participants at each tender and lower price levels. For operators of industrial energy system especially aFRR and mFRR are of economic interest, since the prequalification is very similar and at each there are two ways to increase their income or at least reduce their expenses. The minimum and incremental size of each bid at the power tender is 1 MW, which leads to a minimum capacity of industrial energy systems have to be part of the balancing market. Due to companies like nextKraftwerk, which are so called aggregators, this issue is solved and operators of smaller generation units can be part of the balancing market. In the following Table 4 all balancing service providers and their prequalification status of each level

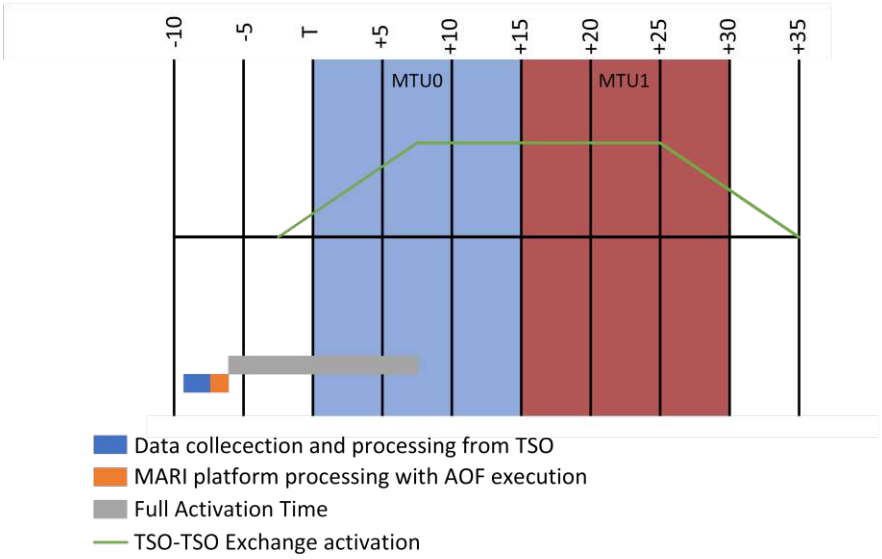

Figure 12: *Direct activation in MARI [14].*

of the balancing market is listed.

2.4 Intervene of transmission system operators

While balancing energy is required to manage unpredictable frequency deviations, redispatch is a forward-looking network management mechanism to prevent congestion in power grids. To understand the scheme behind redispatch, the term dispatch is introduced. All suppliers of electrical energy must provide APG a schedule of their facilities for the next day. This schedule is based on economic parameters, so that each supplier achieves the highest possible profits, the so called dispatch. APG calculates a load flow calculation with the given data and creates a feed-in feed-out forecast for grid levels. Due to this information APG orders power plant operators to postpone planned electricity production, to prevent congestion in the power grid; known as redispatch. In recent years, the costs for these redispatches have risen, which is due to both the energy transformation to volatile renewable ones and sluggish grid expansion.

Table 4: *List of prequalificated Balancing service providers [8].*

Balancing service provider	FCR	aFRR	mFRR
A1 Telekom Austria AG		X	X
Energie AG Oberösterreich Kraftwerke GmbH	X	X	
EVN AG	X	X	X
GEN-I Vienna GmbH		X	X
KELAG-Kärntner Elektrizitäts-Aktiengesellschaft	X	X	X
Lechwerke AG		X	X
Linz Strom GmbH			X
Next Kraftwerke GmbH		X	X
Norske Skog Bruck GmbH*			
ÖBB-Infrastruktur AG		X	X
TIWAG-Tiroler Wasserkraft AG	X	X	X
Salzburg AG für Energie, Verkehr und Telekommunikation	X	X	X
VERBUND Energy4Business GmbH	X	X	X
VERBUND Energy4Flex GmbH	X	X	X
illwerke vkw AG		X	X
Wien Energie GmbH		X	X

3 Methods

This chapter starts with fundamental hypothesis, where the knowledge presented in Section 2.3 is summarised and conclusions with an impact of the optimisation are drawn. The two stages of the mixed integer linear programming (MILP) optimisation and the stochastic approach are introduced the following section. Forecast and historical input data, like the electricity price prediction using a NARX neural network, the historical levels of acceptance probability of the capacity tender, the calculation of the photovoltaic coefficient by historical data and the price levels of the energy market are presented in the next section. In the last two sections are the MILP implementation of the industrial energy system and the balancing energy market are introduced.

3.1 Fundamental hypothesis

As described in Chapter 2 the balancing energy market is divided in three levels Frequency Containment Reserve, automatic frequency restoration reserves and manual frequency restoration reserves. While FCR only consists of a capacity tender, aFRR and mFRR are split in a capacity as well as an energy tender. At capacity tender the bid of a balancing service provider can be accepted or declined. If the bid gets accepted, the BSP gets refunded for providing the offered capacity. The highest refunds are paid for the FCR, the lowest for the mFRR. If a Bid is accepted at the capacity tender, a bid for the corresponding time in the energy tender has to be offered. There each bid can be called, if it is required to keep the grid frequency in its limits ($50.0 \pm 0.2\,\mathrm{Hz}$). The highest called bid determines the price, as it is explained in Section 2.3. As listed in Chapter 2 there are different prequalification requirements for each level of balancing energy. The prequalification for FCR is the toughest one, in terms of activation time, technical requirements and information technology. Due to the huge amount of effort needed from a BSP to take part of the FCR tenders, their economic impact to industrial energy systems is not further investigated in this thesis. Prequalification for aFRR and mFRR differs

very little. Since MARI will be implemented in this year, and the mFRR market is due to the changed bidding scheme (direct and scheduled activation), as described in Subsection 2.3.3 extremely complex to model, aFRR-market is considered to be the most insightful one. It is assumed that the electrical energy storage of the IES is prequalified, the maximum capacity offered is determined by the capacity of the electrical energy storage. If a certain capacity is offered in the capacity bid, the maximum charging and discharging rate is reduced over the duration of the tender. Thus, it is possible to retrieve the offer in the energy tender. Additional linear charge and discharging characteristic are assumed.

3.2 Structure of the optimisation code

In order to represent both the capacity and the energy market of aFRR, the concept of multi-stage optimization is used here. At stage one the optimal schedule of the given industrial energy system with respect to capacity tender is calculated. Which is influenced by an energy price prediction, as well as different levels of acceptance. The used forecast data and their calculation is shown in Section 3.3. Stage two obtains information about the real day ahead price as well as the information if the offered bids are accepted. So the in stage one calculated schedule can be adapted, with respect the electric energy bought and sold in stage one. Since it is very hard to predict the amount of called up energy and its corresponding compensation, the average energy price as well as the retrieved amount is used to calculate the possible revenues. A general overview from the stages and all data sets are shown in Figure 13. Since it is possible for a BSP to offer more than one bid, different scenarios can occur. Each bid can either be accepted or declined, in the case of one bid this leads to two different scenarios, but in case of four bids 16 different scenarios are possible to occur. In order to keep the amount of possible scenarios as small as possible, bids for positive and negative balancing energy are considered separately. A decision tree for two bids is shown in Figure 14.

Each scenario has a certain likelihood of occurrence S_{LoO}, which is determined by the level of acceptance probability B_{LAP} of each bid and the amount of different Bids. The acceptance probability is based on the asking price from the BSP for the corresponding Bid. If the BSP requested a low price for one bid, it is more likely to be accepted by APG, and vice versa for high prices.The considered price levels in this optimisation are shown in Section 3.3.2.

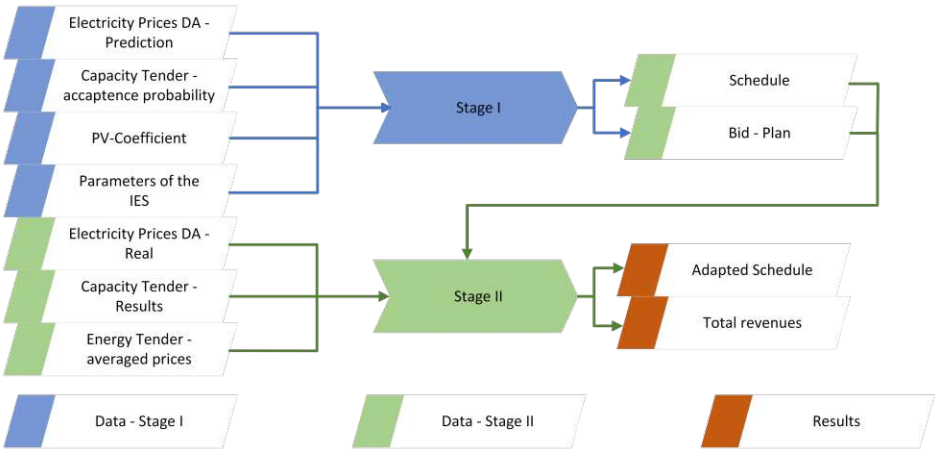

Figure 13: *Stage overview of the optimisation.*

Additional to the likelihood of occurrence of the scenarios, each of them have a expected value of revenues S_{EVR}, which describes the revenues the BSP receives if his bid got accepted. The expected value of revenues, is determined by the size of the bid and the price level. By multiplying the likelihood of appearance of each scenarios with it's corresponding expected value of revenues the expected revenues of the positive and the negative aFRR balancing energy is obtained as it is shown in Equation 1.

$$R_{VE,cap} = S_{LoO} \cdot S_{EVR} \tag{1}$$

$$S_{LoO,1} = B_{LAP,1} \cdot B_{LAP,2} \tag{2}$$

$$S_{LoO,2} = B_{LAP,1} \cdot (1 - B_{LAP,2}) \tag{3}$$

$$S_{LoO,3} = (1 - B_{LAP,1}) \cdot B_{LAP,2} \tag{4}$$

$$S_{LoO,4} = (1 - B_{LAP,1}) \cdot (1 - B_{LAP,2}) \tag{5}$$

3.3 Forecast and historical input data

This section deals with all the data needed for the mentioned model structures. These are, the day ahead electricity price forecast, the acceptance probability and the corresponding prices for the capacity tender, the calculation of the revenues of the energy tender and the photovoltaic efficiency coefficient. In the following each data set is explained as well as the used method. All data used in this thesis are based on open source.

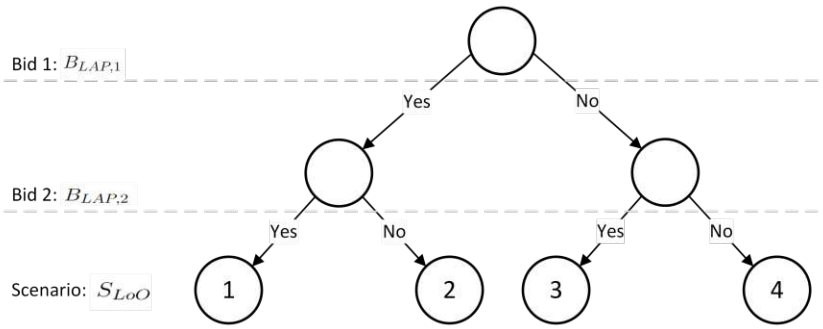

Figure 14: *Different scenarios of acceptance for the capacity tender.*

3.3.1 Day-ahead electricity price forecast using a NARX neural net

Predicting electricity prices for the next day is complex as it depends on many different aspects, such as weather conditions, commodity prices, and consumption and demand, as well as politics to name a few. In this thesis a nonlinear autoregressive neural network with external input is used to predict the electricity price of the next 24 hours in hourly time steps. Therefore generation forecast and DA-prices from 2020 to 2022 are used to train and validate the neural network. These data are exported from the transparency platform of ENTSO-e. Out of the given generation forecast the change per time-step can be evaluated, so it can be used as an input parameter. The price data have been shifted to obtain values for the last day, last week and two, three and four weeks before, as it is shown in in Table 5. There $g(T)$ indicates generation and $p(T)$ is used for price related parameters and $-X$ describes the amount of hours which are shifted. All the data is divided in training and testing data according to 85 % to 15 %. The neural network uses six input and feedback delays and ten neurons in the hidden layer. As training function Bayesian regularisation back propagation is used [15]. The structure of the neural network is shown in Figure 15. It is used to predict the electricity prices of January and the beginning of February of 2023. Out of these prediction three days are observed in more detail as shown in Figure 16. In the further Optimisation $A_{DA,pred}$ is used for the predicted data and $A_{DA,real}$ describe the real day-ahead prices.

3.3.2 Historical price levels of the aFRR capacity tender

The capacity tender consists of six four hour blocks for each, positive and negative capacity. All accepted offers, including their size and their revenue level are published by APG as well as on the transparency platform of ENTSO-e. Since there is a huge

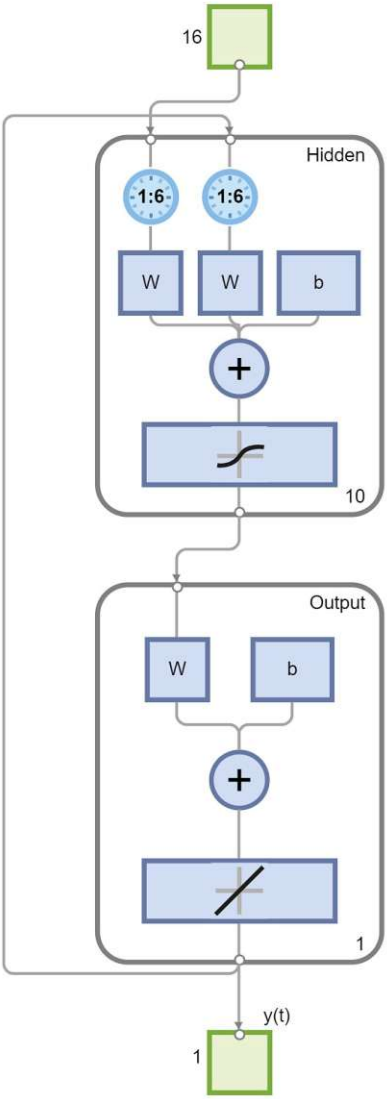

Figure 15: *NARX neural network view.*

Table 5: *Parameters of the NARX neural network*

Input nr.	Description	Inputs	Relation
1 Time information	Day of week	1	
2	Time slot	1	T
3 Load forecast	Forecast Generation	1	$g(T)$
4	Forecast Change	1	$g(T) - g(T-1)$
5 Price information	one day ago	5	$p(T-22)$, $p(T-23)$, $p(T-24)$, $p(T-25)$, $p(T-26)$,
6	one week ago	3	$p(T-167)$, $p(T-168)$, $p(T-169)$
7	two weeks ago	1	$p(T-336)$
8	three weeks ago	1	$p(T-504)$
9	four weeks ago	1	$p(T-672)$

deviation in the capacity price over a year, the exported data from January the 1. of 2022 to January the 31. of 2023, is split monthly. In the next step the confidence intervals of the expected value of revenues, for each time slot, are calculated. In this thesis 20 %, 40 %, 60 % and 80 % are chosen. Additionally the level for 0 % is defined with the maximum price which can be requested, and a 100 % level is implemented through zero revenues. These two levels are needed to generate the possibility of not offering an bid. This leads to $A_{cap,rev}$, a matrix with dimension $6 \times 6 \times 13$. Where the first dimension are the amount of time slots, the second one describes the amount of levels of acceptance and the last dimension are the amount of considered months. In the further optimisation, one explicit month can be selected, which reduces the dimension to a 6×6 matrix. since the data contains only accepted bids, these values correspond inversely to the acceptance probability. The corresponding revenues of the acceptance probability is defined as $B_{LAP,VER}$. In Figure 17 the corresponding revenues to an acceptance of 40% over one year are shown. As it can be seen the revenues for negative and positive differ over the year.

3.3.3 Photovaltaic coefficient

The used photovoltaic-coefficient, describes the time depending efficiency. If this value reaches one, the photovoltaic plant reaches its installed capacity also known as peak power. To obtain this value, the total energy generated by solar plants in Austria in 2022 is exported by ENTSO-e. Then data is split monthly, and divided trough the highest generated power in this year. From each month the average

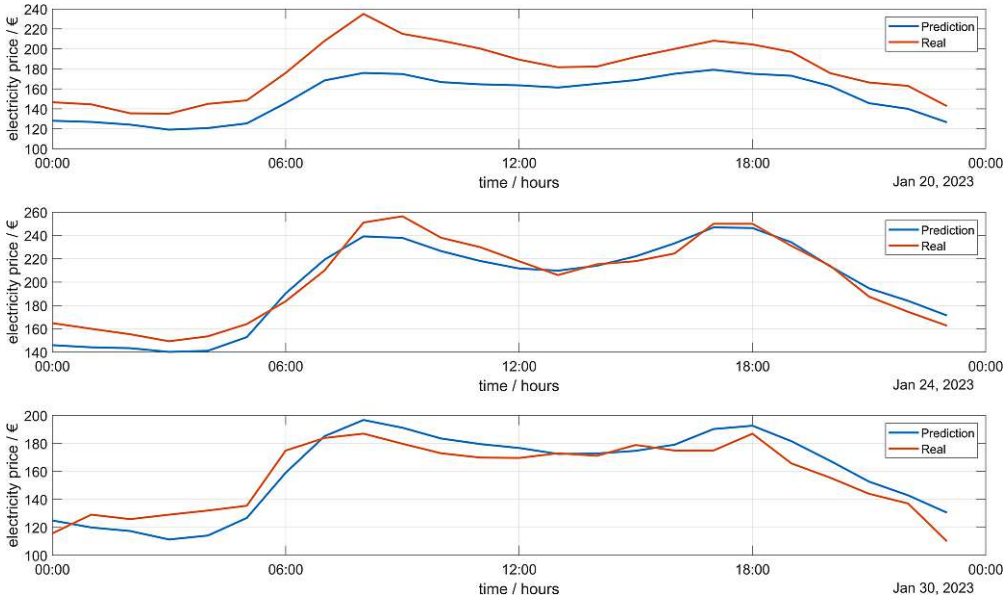

Figure 16: *Electricity price prediction and real day-ahead prices for 20th, 24th and 30th of January.*

efficiency value is used lleading to $A_{PV,coeff}$. These curves are shown in the following Figure 18. In order to make the illustration clearer, it has been divided into two parts: the left-hand illustration shows the months from January to June, while the right-hand illustration shows the months from July to December.

3.3.4 Averaged historical price of the aFRR energy tender

The retrieved amount of balancing energy is unpredictable, which leads to strong fluctuating price levels. Additionally PICASSO is implemented in Austria, but not in the complete European electricity market design, so its total influence is hard to predict. Due to the above mentioned reasons, historical data from ENTSO-e is used. Additional the offered price is determined by the balancing service provider, in this case the proprietor of the industrial energy system. This allows to choose a bid price in order to make a profit in any case. In this optimisation, the average compensation for each time-step and month is used to calculate possible revenues $A_{energy,rev}$.

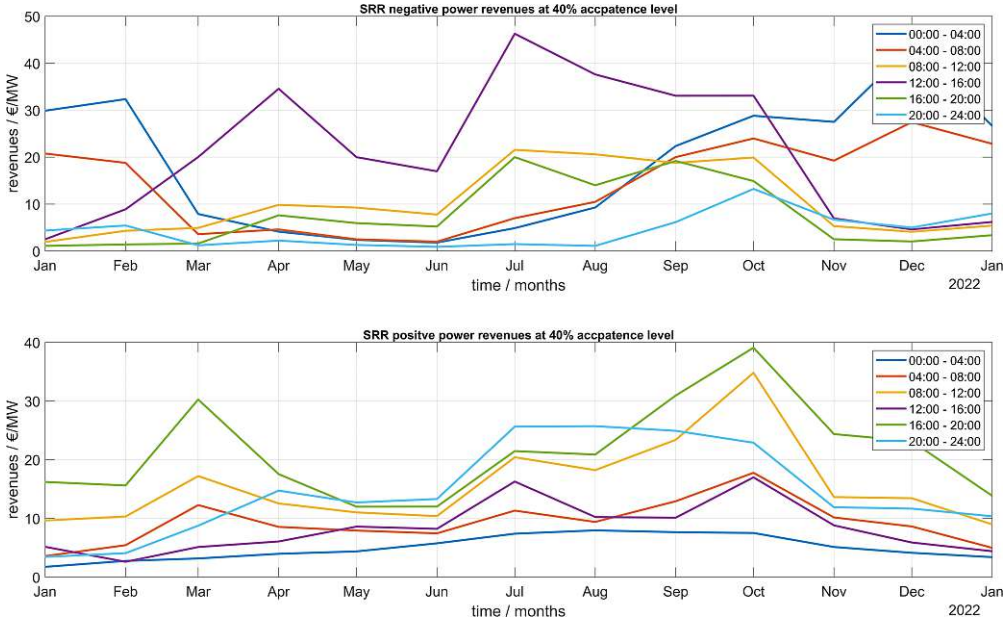

Figure 17: *Corresponding revenues for positive and negative aFRR capacity at an acceptance level of* 40%.

3.4 MILP implementation of the IES

In order to verify the formulation and implementation of the balancing energy market a use case was created for this purpose. This use case, consists of a combined heat and power plant, an electrode boiler, a photovoltaic system, a thermal and a electric energy storage. The parameters, the variables and mixed integer linear programming (MILP) formulation of these energy system are described in the following section. Since the use case assumed here is an industrial plant an electric as well as a thermal demand have to be fulfilled.

3.4.1 Time discretisation

Time discretisation is an important part of optimization. If the discretisation is too fine, this has a negative effect on the computing time, while a discretisation that is too coarse produces less accurate results. Several different time resolutions are possible here, for example, the capacity tender is relevant for 4-hour blocks, the electricity drawn from the grid is billed in hourly prices, the control energy actually called up is remunerated on a four second basis and the results are published in quarter hours, and technical systems operate in even shorter time intervals. To obtain acceptable results with adequate computing time one day is split up to

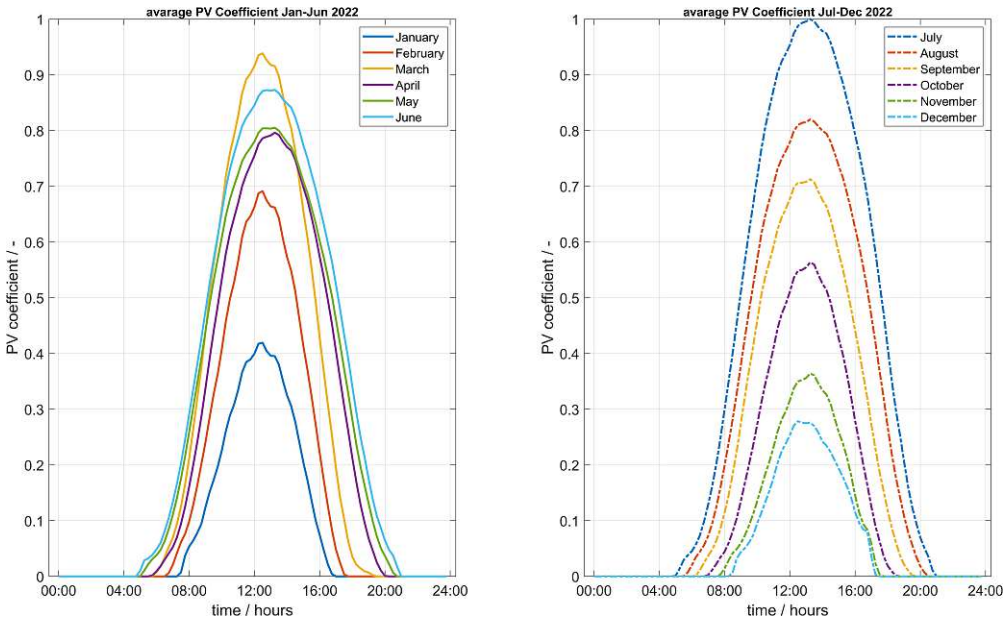

Figure 18: *Average values of the PV coefficient from 2022.*

96 time slots, which means every slot corresponds to 15 minutes. Leading to the parameters shown in Table 6.

Table 6: *Parameters of the time discretisation.*

Parameter	Description	Unit	Value
T_0	Start time	h	0
T	End time	h	24
n	Time steps	–	96
ΔT	Size of each time step	h	0.25

3.4.2 Combined heat and power plant

A combined heat and power plant (CHP) delivers thermal as well as electric power. The CHP plant modelled operates in a range of minimum Power $P_{CHP,min}$ to maximum Power $P_{CHP,max}$. Since electric as well as thermal power is generated, two different energy conversion efficiencies have to be defined, $\eta_{elctric}$ and $\eta_{thermal}$, both of them are assumed to be constant. The maximum gradient of the CHP plant is limited trough $P_{CHP,maxGrad}$, which prevents the power plant from a heavily oscillating usage. In addition, a minimum on/off time is specified, which describes a period of time needed to start the CHP unit after shutdown or vice versa. These are

represented by $t_{CHP,minOn}$ and $t_{CHP,minOff}$. The energy content of the fuel H_l as well as the constant fuel price c_l is also needed. All parameters are specified in Table 7. In Table 8 the required variables, for the MILP formulation are listed. The total

Table 7: *Parameters of the combined heat and power plant.*

Parameter	Description	Unit	Value
$P_{CHP,min}$	Minimum power	MW	6
$P_{CHP,max}$	Maximum power	MW	18
$\eta_{CHP,el}$	Electric efficiency	–	0.35
$\eta_{CHP,th}$	Thermal efficiency	–	0.25
$P_{CHP,maxGrad}$	Maximum power gradient	MW/h	5
$t_{CHP,minOn}$	Minimum operating time	h	2
$t_{CHP,minOff}$	Minimum stagnation time	h	2
H_l	energy content	kWh/kg	15
c_l	fuel price	€/kg	1.65

power consumption P_{CHP} of the CHP have to be between $\{0, P_{CHP,min}P_{CHP,max}\}$. This is obtained by the formulation shown in Equation 6 and Equation 7. The binary variable b_{CHP}, the so-called on/off status is needed to realise a semi-continuous operating state. Fuel consumption can not be negative, since the CHP is not able to produce fuel, indicated in Equation 8. The correlation between P_{CHP}, m_{fuel} and H_l is given in Equation9. Electric and thermal power generated are based on their respective efficiency parameter, as it can be seen in Equation 10 and Equation 11. The calculation of the change-rate as well as the switching is shown from Equation 12 to Equation 15.

Table 8: *Variables of the combined heat and power plant.*

Variable	Description	Unit	Dimension
P_{CHP}	Total power consumption	MW	$\mathbb{R}^{n\times 1}$
b_{CHP}	On/Off status	–	$\{0,1\}^{n\times 1}$
m_{fuel}	fuel consumption	kg	$\mathbb{R}^{n\times 1}$
$P_{CHP,el}$	Electric power generated	MW	$\mathbb{R}^{n\times 1}$
$P_{CHP,th}$	Thermal power generated	MW	$\mathbb{R}^{n\times 1}$
$P_{CHP,change}$	Change of total power consumption	MW/h	$\mathbb{R}^{n\times 1}$
s_{CHP}	On/Off switching	–	$\{-1,0,1\}^{n\times 1}$

$$P_{CHP_i} \geq P_{CHP,min_i} \cdot b_{CHP_i} \qquad \forall i \in \{1,...,n\} \tag{6}$$

$$P_{CHP_i} \leq P_{CHP,max_i} \cdot b_{CHP_i} \qquad \forall i \in \{1, ..., n\} \tag{7}$$

$$m_{fuel_i} \geq 0 \qquad \forall i \in \{1, ..., n\} \tag{8}$$

$$P_{CHP_i} = m_{fuel_i} \cdot H_l \qquad \forall i \in \{1, ..., n\} \tag{9}$$

$$P_{CHP,el_i} = P_{CHP_i} \cdot \eta_{CHP,el} \qquad \forall i \in \{1, ..., n\} \tag{10}$$

$$P_{CHP,th_i} = P_{CHP_i} \cdot \eta_{CHP,th} \qquad \forall i \in \{1, ..., n\} \tag{11}$$

$$P_{CHP,change_i} = \frac{P_{CHP_i} - P_{CHP_{i-1}}}{\Delta T} \qquad \forall i \in \{2, ..., n\} \tag{12}$$

$$P_{CHP,change_1} = \frac{P_{CHP_1} - P_{CHP_n}}{\Delta T} \tag{13}$$

$$s_{CHP,change_i} = \frac{b_{CHP_i} - b_{CHP_{i-1}}}{\Delta T} \qquad \forall i \in \{2, ..., n\} \tag{14}$$

$$s_{CHP,change_1} = s_{CHP,change_n} \tag{15}$$

3.4.3 Electrode boiler

The electrode boiler operates continuously in a range from $P_{boiler,min}$ to $P_{boiler,max}$. The efficiency from electric to thermal energy is η_{boiler}. In contrast to the CHP, there is no minimum operating or stagnation time, additionally there are no restrictions regarding the gradient. All parameters, including their value and their corresponding unit, are shown in Table 9. Table 10 shows all necessary variables

Table 9: *Parameters of the electrode boiler.*

Parameter	Description	Unit	Value
$P_{boiler,min}$	Minimum power	MW	0
$P_{boiler,max}$	Maximum power	MW	8
η_{boiler}	Efficiency	–	0.95

for MILP formulation of the electrode boiler. $P_{boiler,el}$ is the variable of the electric consumption, while $P_{boiler,th}$ describes the thermal power output, they are connected via the efficiency η_{boiler}, given in Equation 16. Additionally the electric consumption is limited trough $P_{boiler,min}$ and $P_{boiler,min}$, indicated in Equation 17 and Equation

18.

Table 10: *Variables of the electrode boiler.*

Variable	Description	Unit	Dimension
$P_{boiler,el}$	Electric power consumption	MW	$\mathbb{R}^{n\times1}$
$P_{boiler,th}$	Thermal power generation	MW	$\mathbb{R}^{n\times1}$
b_{boiler}	On/Off status	–	$\{0,1\}^{n\times1}$

$$P_{boiler,th_i} = P_{boiler,el} \cdot \eta_{elctric} \qquad \forall i \in \{1,...,n\} \tag{16}$$

$$P_{boiler,el_i} \geq P_{boiler,min_i} \cdot b_{boiler_i} \qquad \forall i \in \{1,...,n\} \tag{17}$$

$$P_{boiler,el_i} \leq P_{boiler,max_i} \cdot b_{boiler_i} \qquad \forall i \in \{1,...,n\} \tag{18}$$

3.4.4 Photovoltaic system

Electric energy generated by the photovoltaic system is determined by weather conditions, and the used area, these are expressed trough the parameters shown in Table 11. The used parameters are the generated power of the photovoltaic system P_{PV}, area cover by PV-panels A_{PV} and peak power per square-meter. The selected data used to describe the efficiency of the photovoltaic system are explained in Section 3.3, and is defined as $A_{PV,coeff}$. The correlation between P_{PV}, $P_{PV,peak}$, A_{PV} and $A_{PV,coeff}$ is given by Equation 19.

Table 11: *Parameter of the photovoltaic system.*

Parameter	Description	Unit	Value
$P_{PV,peak}$	Peak power per m^2	kWp/m^2	0.2
A_{PV}	covered PV-area	m^2	15 000
$A_{PV,coeff}$	calculated efficiency coefficient	kW/kWp	
P_{PV}	PV-power generation	MW	

$$P_{PV_i} = P_{PV,peak} \cdot A_{PV} \cdot A_{PV,coeff_i} \qquad \forall i \in \{1,...,n\} \tag{19}$$

3.4.5 Thermal energy storage

A thermal energy storage (TES) system is determined by two governing parameters, on the one hand the capacity $C_{TES,min}$ and $C_{TES,max}$, and on the other with the

charge/discharge-rate $F_{TES,C}$ and $F_{TES,DC}$. These parameters are listed in Table 12. In Table 13 the level of the TES L_{TES} as well as the flow from or to the TES

Table 12: *Parameters of the thermal energy storage.*

Parameter	Description	Unit	Value
$C_{TES,min}$	Minimum capacity	MWh	0
$C_{TES,max}$	Maximum capacity	MWh	6
$F_{TES,C}$	Maximum charge rate	MW	1
$F_{TES,DC}$	Maximum discharge rate	MW	1

F_{TES} are listed. The level of the TES is constrained by the minimum and maximum capacities $C_{TES,min}$ and $C_{TES,min}$, shown in Equation 20 and 21. As determined in Equation 22 and 23. Additionally the flow variable is restricted by $F_{TES,C}$ and $F_{TES,DC}$ shown by the Equations 24 and 25 .

Table 13: *Variables of the thermal energy storage.*

Variable	Description	Unit	Dimension
L_{TES}	Level of the TES	MWh	$\mathbb{R}^{n\times 1}$
F_{TES}	Flow from/to TES	MW	$\mathbb{R}^{n\times 1}$

$$L_{TES_i} \geq C_{TES,min} \qquad \forall i \in \{1, ..., n\} \tag{20}$$

$$L_{TES_i} \leq C_{TES,max} \qquad \forall i \in \{1, ..., n\} \tag{21}$$

$$L_{TES_i} = L_{TES_{i-1}+L_{TES_{i-1}}\cdot\Delta T} \qquad \forall i \in \{2, ..., n\} \tag{22}$$

$$L_{TES_1} = L_{TES_n} + L_{TES_n} \cdot \Delta T \tag{23}$$

$$F_{TES_i} \leq F_{TES,C} \qquad \forall i \in \{1, ..., n\} \tag{24}$$

$$F_{TES_i} \leq F_{TES,DC} \qquad \forall i \in \{1, ..., n\} \tag{25}$$

3.4.6 Electric energy storage

Since a electric energy storage (EES) is also determined by the capacity $C_{EES,min}$ and $C_{EES,max}$, as well as with the charge/discharge-rate $F_{EES,C}$ and $F_{EES,DC}$, these parameters are listed in Table 14. Table 15 lists the level of the EES L_{EES} as well

Table 14: *Parameters of the electric energy storage.*

Parameter	Description	Unit	Value
$C_{EES,min}$	Minimum capacity	MWh	0
$C_{EES,max}$	Maximum capacity	MWh	12
$F_{EES,C}$	Maximum charge rate	MW	4
$F_{EES,DC}$	Maximum discharge rate	MW	4

as the flow from or to the EES F_{EES}. The level is constrained by the minimum and maximum capcities $C_{EES,min}$ and $C_{EES,min}$, shown in Equation 26 and 27. The level of the EES is determined by Equation 28 and 29. Additionally the flow variable is restricted by $F_{EES,C}$ and $F_{EES,DC}$ shown by the Equations 30 and 31.

Table 15: *Variables of the electric energy storage.*

Variable	Description	Unit	Dimension
L_{EES}	Level of the EES	MWh	$\mathbb{R}^{n\times 1}$
F_{EES}	Flow from/to EES	MW	$\mathbb{R}^{n\times 1}$

$$L_{EES_i} \geq C_{EES,min} \qquad \forall i \in \{1, ..., n\} \tag{26}$$

$$L_{EES_i} \leq C_{EES,max} \qquad \forall i \in \{1, ..., n\} \tag{27}$$

$$L_{EES_i} = L_{EES_{i-1}} + L_{EES_{i-1}} \cdot \Delta T \qquad \forall i \in \{2, ..., n\} \tag{28}$$

$$L_{EES_1} = L_{EES_n} + L_{EES_n} \cdot \Delta T \tag{29}$$

$$F_{EES_i} \leq F_{EES,C} \qquad \forall i \in \{1, ..., n\} \tag{30}$$

$$F_{EES_i} \geq F_{EES,DC} \qquad \forall i \in \{1, ..., n\} \tag{31}$$

3.4.7 Electricity grid

To limit the energy from and to the grid, the electricity grid is formulated. Therefore two parameter $P_{fG,max}$ and $P_{tG,max}$ are defined. Additionally the variables $b_{buy,DA}$ and $b_{sell,DA}$ prevent arbitrage deals shown in Equation 32. Since the energy have to consumed or delivered for one hour, $b_{buy,DA,n}$ and $b_{sell,DA,n}$ are introduced which map $b_{buy,DA}$ and $b_{sell,DA}$ to the used discrete time grid, shown in Equation 33 and Equation 34. Due to Equation 35 and Equation 36 the limits are adhered by P_{fG} and P_{tG}. All parameters used are listed in Table 16 and all variables are shown in Table 17.

Table 16: *Parameters of the electric grid.*

Variable	Description	Unit	Value
$P_{fG,max}$	Maximum power from grid	MW	10
$P_{tG,max}$	Maximum power to grid	MW	10

Table 17: *Variables of the electric grid.*

Variable	Description	Unit	Dimension
$b_{buy,DA}$	Buy decision - 24 time-steps	-	$\{0,1\}^{T\times 1}$
$b_{sell,DA}$	Sell decision - 24 time-steps	-	$\{0,1\}^{T\times 1}$
$b_{buy,DA,n}$	Buy decision - 96 time-steps	-	$\{0,1\}^{n\times 1}$
$b_{sell,DA,n}$	Sell decision - 96 time-steps	-	$\{0,1\}^{n\times 1}$
P_{fG}	Power from the grid	MW	$\mathbb{R}^{n\times 1}$
P_{tG}	Power to the grid	MW	$\mathbb{R}^{n\times 1}$

$$b_{buy,DA_j} + b_{sell,DA_j} \leq 1 \qquad : \forall j \in \{1,...,T\} \tag{32}$$

$$b_{buy,DA,n_{4(j-1)+1:4j}} = b_{buy,DA_j} \qquad : \forall j \in \{1,...,T\} \tag{33}$$

$$b_{sell,DA,n_{4(j-1)+1:4j}} = b_{sell,DA_j} \qquad : \forall j \in \{1,...,T\} \tag{34}$$

$$0 \leq P_{fG_i} \leq P_{fG,max} \qquad : \forall i \in \{1,...,n\} \tag{35}$$

$$0 \leq P_{tG_i} \leq P_{tG,max} \qquad : \forall i \in \{1,...,n\} \tag{36}$$

3.4.8 Electric and thermal demand

In this subsection the electric and the thermal demand for the industrial energy system are specified. Each of them has a base value, which is 20% of the peak

demand $P_{dem,el,peak}$ and $P_{dem,th,peak}$. The electric demand $P_{dem,el}$ is given by the Equation 37 and the thermal one $P_{dem,th}$ in Equation 38, whereas t is the given time-vector. Since the electricity as well as the thermal demand has to be full filled at every time, Equation 39 and Equation 40 have to be met. In Equation 40 the waste heat $P_{wasteHeat}$ is introduced, which is used as a soft constraint, so that it is possible to produce more thermal energy than needed. All used parameters are listed in Table 18.

Table 18: *Parameters of the electric and thermal demand.*

Variable	Description	Unit	Value
$P_{dem,el,peak}$	Electric peak demand	MW	10
$P_{dem,th,peak}$	Thermal peak demand	MW	10
$P_{dem,el}$	Electric demand	MW	–
$P_{dem,th}$	Thermal demand	MW	–

$$P_{dem,el} = P_{dem,el,peak} \cdot \left(0.2 + 0.8 \cdot \frac{1 - \cos\left(\frac{t}{t(n) + \Delta T} \cdot 4\pi \right)}{2} \right) \tag{37}$$

$$P_{dem,th} = P_{dem,th,peak} \cdot \left(0.2 + 0.8 \cdot \frac{1 - \cos\left(\frac{t}{t(n) + \Delta T} \cdot 2\pi \right)}{2} \right) \tag{38}$$

$$P_{fG_i} + P_{CHPel_i} + P_{PV_i} = P_{dem,el_i} + P_{boiler,el_i} + P_{tG_i} + F_{EES} \tag{39}$$

$$P_{CHP,th_i} + P_{boiler,th_i} = P_{dem,th_i} + F_{TES} + P_{wasteHeat} \tag{40}$$

3.4.9 Objectives

In this subsection the objective function, necessary variables and constraints are defined. The costs/revenues are determining this optimization, therefore all of them are in the governing objective function. It consists of three parts, the costs for fuel c_{fuel} , the costs $c_{pred,el,DA}$ and the revenues from electricity $r_{pred,el,DA}$, as shown in Equation 41. To obtain these three values the Equations 42 to 44 are needed. Equation 42 calculates the price of the needed fuel, according to the fuel price c_l, which is set constant. Equation 43 and Equation 44 calculate the predicted electricity costs/revenues, according to the forecast from Subsection 3.3.1. To archive the real costs/revenues $c_{real,el,DA}$ and $r_{real,el,DA}$ Equation 45 and 46 are used. The variables

are shown in Table 19.

$$obj = \sum_{i}^{T} c_{fuel}(i) + \sum_{i}^{T} C_{pred,el,DA}(i) - \sum_{i}^{T} R_{pred,el,DA}(i) \tag{41}$$

$$c_{fuel_i} = c_l \cdot m_{fuel_i} \cdot \Delta T \qquad : \forall i \in \{1, ..., n\} \tag{42}$$

$$c_{pred,el,DA_i} = P_{fG_i} \cdot A_{DA,pred_i} \cdot \Delta T \qquad : \forall i \in \{1, ..., n\} \tag{43}$$

$$r_{pred,el,DA_i} = P_{tG_i} \cdot A_{DA,pred_i} \cdot \Delta T \qquad : \forall i \in \{1, ..., n\} \tag{44}$$

$$c_{real,el,DA_i} = P_{fG_i} \cdot A_{DA,real_i} \cdot \Delta T \qquad : \forall i \in \{1, ..., n\} \tag{45}$$

$$r_{real,el,DA_i} = P_{tG_i} \cdot A_{DA,real_i} \cdot \Delta T \qquad : \forall i \in \{1, ..., n\} \tag{46}$$

Table 19: *Variables of the objective function.*

Parameter	Description	Unit	Dimension
c_{fuel}	Fuel cost	€	$\mathbb{R}^{n\times1}$
$c_{pred,el,DA}$	Predicted electricity costs	€	$\mathbb{R}^{n\times1}$
$r_{pred,el,DA}$	Predicted electricity revenues	€	$\mathbb{R}^{n\times1}$
$c_{real,el,DA}$	Real electricity costs	€	$\mathbb{R}^{n\times1}$
$r_{real,el,DA}$	Real electricity revenues	€	$\mathbb{R}^{n\times1}$

3.5 MILP implementation of the balancing energy

This section is about the MILP implementation of the balancing capacity and energy tender in the already described industrial energy system. All modelling assumptions are already determined in Section 3.1. Since the capacity tender is done in stage one and the energy tender is performed in stage two of the optimisation, it is meaningful to split their implementation in two subsections.

3.5.1 Capacity tender

In the capacity tender there are four degrees of freedom considered Three of them determine each bid, the chosen time-slot, the level of acceptance probability, the offered amount of capacity. The forth degree of freedom is the amount of bids, since more than one bid is assumed. As already mentioned, there are six different time-slots in each capacity tender of the aFRR. They are from $00:00 - 04:00$,

$04:00-08:00$, $08:00-12:00$, $12:00-16:00$, $16:00-20:00$, $20:00-24:00$. For each capacity tender (positive and negative) an offered bid has to last for at least one entire time-slot. This results in the first parameter T_{Slot}. As explained in Section 3.3 there are different levels of acceptance probability B_{AP}, 100 %, 80 %, 60 %, 40 %, 20 %, 0 %, their total number is designated by B_{LAP}. Each of those levels determines the corresponding price level, which is important for the calculation. The amount of capacity, for each bid is limited through the prequalified capacity which leads to the third parameter P_{preq}. The last of the governing parameters defines the amount of different bids, $A_{mB,pos}$ and $A_{mB,neg}$. A_{mB} is used for both cases in sake of simplicity. All these parameter's are shown in Table 20.

Table 20: *Parameters of the aFRR design.*

Parameter	Description	Unit	Value
T_{Slot}	Number of different time-slots in the capacity tender	-	6
B_{LAP}	Levels of acceptance probability	-	6
P_{preq}	Prequalified capacity of the BSP	MW	6
A_{mB}	Amount of different bids	-	2

In the following, the four-dimensional capacity-tender decision-variables $b_{cap,pos}$ and $b_{cap,neg}$ are introduced, the are visualised in Figure 19 and described in Table 21. The term b_{cap} designates, that the constraint is used for both variables. The four dimensions of the variables are, the already introduced parameters of the energy tender T_{Slot}, B_{LAP}, P_{preq} and A_{mB}. Equation 47 is needed to obtain just one non zero entry in each level of the two-dimensional matrix (time-slot over levels of acceptance probability). Equation 48 ensures that all bids corresponding to one time slot are in the same level of acceptance.

Table 21: *Variables of the aFRR design.*

Variable	Description	Dimension
$b_{cap,pos}$	Positive capacity-tender decision-variables	$\{0,1\}^{T_{slot}\times B_{LAP}\times P_{preq}\times A_{mB}}$
$b_{cap,neg}$	Negative capacity-tender decision-variables	$\{0,1\}^{T_{slot}\times B_{LAP}\times P_{preq}\times A_{mB}}$

$$\sum_{i=1}^{T_{slot}}\sum_{j=1}^{B_{LAP}} b_{cap_{k,l}}(i,j) \leq 1 \quad : \forall k \in \{1,...,P_{preq}\} \wedge \forall l \in \{1,...,A_{mB}\} \tag{47}$$

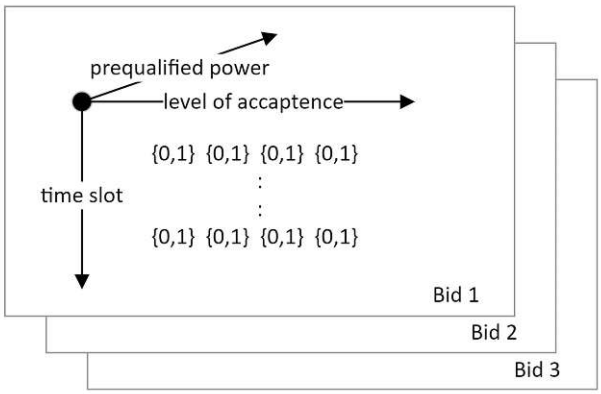

Figure 19: *Visualisation of the 4-dimensional power tender decision-variable.*

$$\sum_{i=1}^{T_{slot}} \sum_{j=1}^{B_{LAP}} b_{cap_{k,l}}(i,j) \leq b_{cap_{k,l}}(i-1,j) \quad : \forall k \in \{2,...,P_{preq}\} \wedge \forall l \in \{1,...,A_{mB}\} \tag{48}$$

To be able to offer a bid of certain size, the industrial energy system must have enough free capacity. The variables $C_{cap,pos}$ and $C_{cap,neg}$ describe the capacity needed in each of the six time slots of T_{Slot} and is calculated as described in Equation 49. Due to Equation 50 this variable is mapped to the discrete time, furthermore $C_{cap,pos,n}$ and $C_{cap,neg,n}$ describe the free capacity which is needed. This means that, if there is one bid of 1 MW, in the first time step of the bid 4 MWh have to be free while and in the last one just 0.25 MWh remain. To fulfil this demand two additional variables are introduced. The maximum positive capacity which can be provided at each time step $C_{in,pos}$ and the negative one $C_{in,neg}$. To obtain these values, the maximum and minimum electric power of the CHP at each time step have to be calculated first, this is done in Equation 51 to Equation 54. Since $C_{in,pos}$ is affected by the maximal producible power $P_{CHP,el,max}$ and the actual level of EES L_{EES} and the minimum capacity of the EES $C_{EES,min}$, it is calculated as shown in Equation 55. The possible negative capacity $C_{in,neg}$, depends on the minimal producible power $P_{CHP,el,min}$ an as well on the actual level of EES L_{EES} and the maximum capacity $C_{EES,max}$ as it is shown in Equation 56. Equation 57 and Equation 58 are needed to meet the demand of free capacity. The neccasary variables are listed in Table 22.

Table 22: *Variables for inactive load.*

Variable	Description	Unit	Dimension
$C_{cap,pos}$	Positive capacity needed	MWh	$\mathbb{R}^{T_{slot}\times 1}$
$C_{cap,neg}$	Negative capacity needed	MWh	$\mathbb{R}^{T_{slot}\times 1}$
$C_{in,pos}$	Inactive positive capacity	MWh	$\mathbb{R}^{n\times 1}$
$C_{in,neg}$	Inactive negative capacity	MWh	$\mathbb{R}^{n\times 1}$
$P_{CHP,el,min}$	Minimum electric power generation of CHP	MW	$\mathbb{R}^{n\times 1}$
$P_{CHP,el,max}$	Maximum electric power generation of CHP	MW	$\mathbb{R}^{n\times 1}$

$$C_{cap_i} = \sum_{j=1}^{B_{LAP}} \sum_{k=1}^{P_{preq}} \sum_{l=1}^{A_{mB}} b_{cap_l}(j,k,l) \quad : \forall i \in \{1,...,T_{slot}\} \tag{49}$$

$$C_{cap,n_{(i-1)\cdot 16+1:(i)\cdot 16}} = \sum_{j=1}^{B_{LAP}} \sum_{k=1}^{P_{preq}} \sum_{l=1}^{A_{mB}} b_{cap_l}(j,k,l)\cdot \Delta T \quad : \forall i \in \{1,...,T_{slot}\} \tag{50}$$

$$P_{CHPel,min_i} = P_{CHPel_{i-1}} - \eta_{CHPel}\cdot P_{CHP,maxGrad} \qquad \forall i \in \{2,...,n\} \tag{51}$$

$$P_{CHPel,min_1} = P_{CHPel_n} - \eta_{CHPel}\cdot P_{CHP,maxGrad} \tag{52}$$

$$P_{CHPel,max_i} = P_{CHPel_{i-1}} + \eta_{CHPel}\cdot P_{CHP,maxGrad} \qquad \forall i \in \{2,...,n\} \tag{53}$$

$$P_{CHPel,max_1} = P_{CHPel_n} + \eta_{CHPel}\cdot P_{CHP,maxGrad} \tag{54}$$

$$C_{in,pos_i} = \Delta T\cdot(P_{CHPel,max_i} - P_{CHPel_i}) + (L_{EES} - C_{EES,min}) \qquad \forall i \in \{1,...,n\} \tag{55}$$

$$C_{in,neg_i} = \Delta T\cdot(P_{CHPel_i} - P_{CHPel,min_i}) + (C_{EES,min} - L_{EES}) \qquad \forall i \in \{1,...,n\} \tag{56}$$

$$C_{cap,pos,n_i} \le C_{in,pos_i} \qquad \forall i \in \{1,...,n\} \tag{57}$$

$$C_{cap,neg,n_i} \le C_{in,neg_i} \qquad \forall i \in \{1,...,n\} \tag{58}$$

Additionally to the free capacity, the flow of the electric energy has to be considered. In the considered IES, it is assumed that the energy for the balancing energy market is only transmitted by the battery, therefore the maximum charge and discharge

flow is reduced according to 59 and 60.

$$F_{EES_i} \leq F_{EES,C} - C_{cap,pos,n} \qquad \forall i \in \{1, ..., n\} \tag{59}$$

$$F_{EES_i} \geq F_{EES,DC} + C_{cap,neg,n} \qquad \forall i \in \{1, ..., n\} \tag{60}$$

In Equation 1 the calculation of the expected revenues from the capacity tender $R_{VE,cap}$ is shown. The following explains how this value is composed by linear optimisation, the corresponding scheme is shown in Figure 20. All used parameters are listed in Table 23 and variables are shown in Table 24. The expected revenues from the capacity tender R_{VE} depends on the four dimensions of the decision variable T_{Slot}, B_{LAP}, P_{preq}, A_{mB} and the expected revenues of the corresponding acceptance probability $B_{AP,ER}$.
By multiplying the already introduced decision variable b_{cap} with the expected revenues of the corresponding acceptance probability $B_{AP,ER}$, $B_{EVR,Tslot}$, the expected revenues of each bid and each time slot (from T_{slot}) is obtained. This is shown in Equation 61. In the further calculation, the information of the used time slot is no longer necessary, therefore B_{EVR} the expected revenues of each bid is calculated by building the sum from $B_{EVR,Tslot}$ over all time slots, as it is done in Equation 62.

Table 23: *Parameters for the stochastic approach of the capacity tender.*

Variable	Description	Unit	Dimension/Value
PS	Amount of possible scenarios	-	$2^{A_{mB}}$
S_{LoO}	Likelihood of occurrence for each possible scenario	-	$\mathbb{R}^{A_{mB_1} \times ... \times A_{mB_{PS}}}$
S_{PS}	Possible scenarios	-	$\{0,1\}^{A_{mB} \times PS}$

$$B_{EVR,Tslot} = \sum_{k=1}^{P_{preq}} (b_{cap_l}(k) \cdot rev_{cap}) \cdot \frac{T}{T_{slot}} \tag{61}$$

$$B_{EVR} = \sum_{i=1}^{T_{slots}} B_{EVR,Tslot}(i) \tag{62}$$

As already mentioned above, a stochastic approach is used in this thises to calculate the expected revenues of the capacity tender $R_{VE,cap}$, for this purpose the term of different scenarios is already discussed in Subsection 3.2 . The matrix containing all possible scenarios S_{PS} depends on the amount of different bids A_{mB}, as it is

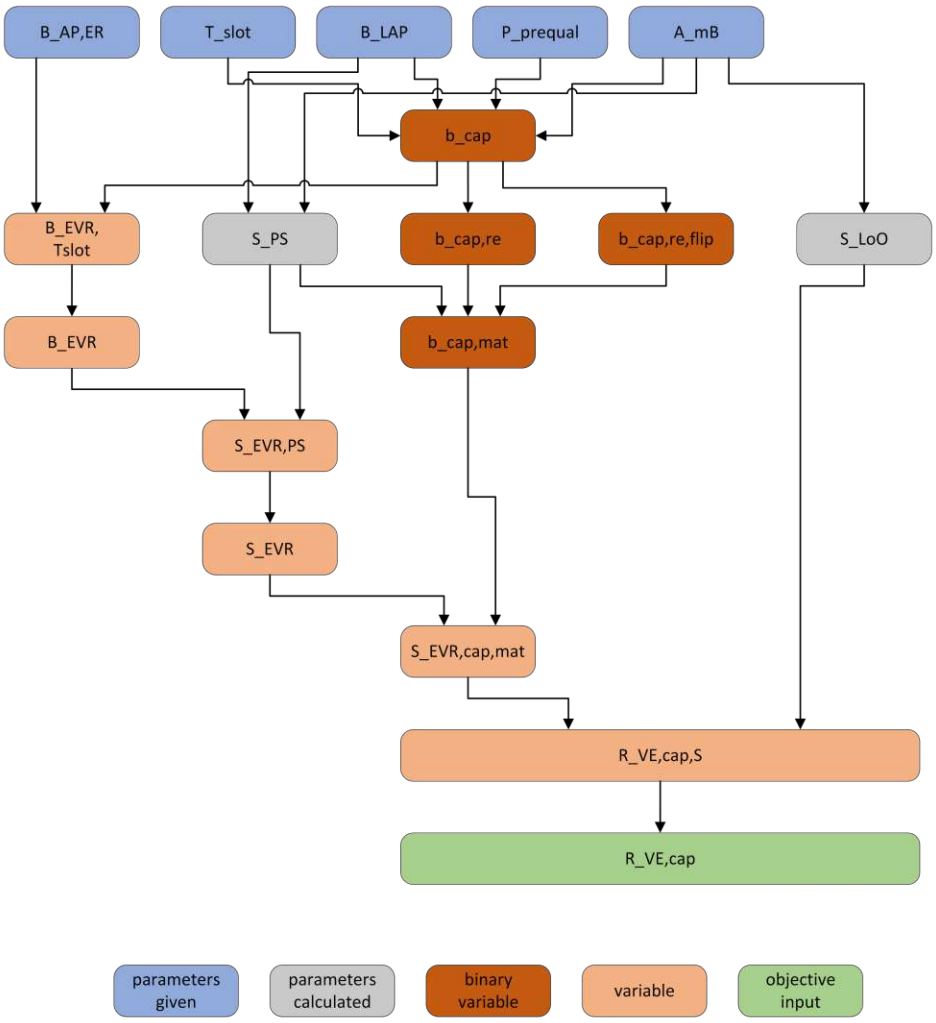

Figure 20: *Visualisation of the calculation of* $R_{VE,cap}$.

visualised for two bids in Equation 63. The amount of rows is equal to the amount of different bids and the amount of rows is corresponding to PS which is further described by the indices $_{PS}$. In Equation 64 the expected revenues of each bid B_{EVR} are multiplied with the possible scenarios S_{PS}, which leads to $S_{EVR,PS}$ the expected revenues of each bid categorised into the possible scenarios. To achieve the expected revenues of each scenario S_{EVR}, the sum over all bids have to be calculated, as shown in 65

$$S_{PS} = \begin{Bmatrix} 1 & 1 & 0 & 0 \\ 1 & 0 & 1 & 0 \end{Bmatrix} \tag{63}$$

Table 24: *Variables for the stochastic approach of the capacity tender.*

Variable	Description	Unit	Dimension
$b_{EVR,Tslot}$	Expected revenues of each bid and each time slot	€	$\mathbb{R}^{T_{slot} \times A_{mB}}$
b_{EVR}	Expected revenues of each bid	€	$\mathbb{R}^{1 \times A_{mB}}$
$S_{EVR,PS}$	Expected revenues of each scenario and time slot	€	$\mathbb{R}^{A_{mB} \times S_{PS}}$
S_{EVR}	Expected revenues of each scenario	€	$\mathbb{R}^{1 \times S_{PS}}$
$b_{cap,re}$	Level of acceptance probability of each bid	-	$\{0,1\}^{A_{mB} \times B_{LAP}}$
$b_{cap,re,flip}$	Level of acceptance probability of each bid	-	$\{0,1\}^{A_{mB} \times B_{LAP}}$
$b_{cap,mat}$	Allocation of each scenario according to S_{LoO}	-	$\{0,1\}^{B_{LAP_1} \times ... \times B_{LAP_{A_{mB}}} \times S_{PS}}$
$S_{EVR,cap,mat}$	Expected revenues allocated according to S_{LoO}	€	$\mathbb{R}^{B_{LAP_1} \times ... \times B_{LAP_{A_{mB}}} \times S_{PS}}$
$R_{VE,cap,S}$	Expected revenues of each scenario weighted by S_{LoO}	€	$\mathbb{R}^{1 \times S_{PS}}$
$R_{VE,cap}$	Expected revenues weighted by S_{LoO}	-	$\mathbb{R}$

$$S_{EVR,PS} = B_{EVR_l} \cdot S_{PS_{l,m}} \quad : \forall l \in \{1, ..., A_{mB}\} \wedge \forall m \in \{1, ..., PS\} \tag{64}$$

$$S_{EVR} = \sum_{j=1}^{A_{mB}} S_{EVR,PS}(j) \tag{65}$$

With S_{EVR} the expected revenues of each scenario are calculated, to be able to calculate $R_{VE,cap}$ the corresponding likelihood of occurrence S_{LoO}, have to be defined. In mixed integer linear programming it is not possible to multiply S_{EVR} with S_{LoO} generated out of the decision variable b_{cap}, another scheme has to be used. Therefore S_{LoO} depends only on the amount of different bids A_{mB} and the different levels of acceptance B_{LAP} and calculates as described in 66. Each dimension of S_{LoO} has B_{LAP} entries and the amount of total dimensions is defined trough A_{mB}. A

visualisation for two bids and six levels of acceptance is shown in 67

$$S_{LoO_{j1,...,j2}} = \prod_{jj}^{A_{mB}} B_{LAP}(jj) \\ : \forall jj \in \{j_1, ..., j_{A_{mB}}\} \wedge \forall \{j_1, ..., j_{A_{mB}}\} \in \{1, ..., B_{LAP}\} \tag{66}$$

$$S_{LoO} = \begin{Bmatrix} 1.00 & 0.80 & 0.60 & 0.40 & 0.20 & 0.00 \\ 0.80 & 0.64 & 0.48 & 0.32 & 0.16 & 0.00 \\ 0.60 & 0.48 & 0.36 & 0.24 & 0.12 & 0.00 \\ 0.40 & 0.32 & 0.24 & 0.16 & 0.08 & 0.00 \\ 0.20 & 0.16 & 0.12 & 0.08 & 0.04 & 0.00 \\ 0.00 & 0.00 & 0.00 & 0.00 & 0.00 & 0.00 \end{Bmatrix} \tag{67}$$

To be able to use matrix calculation S_{EVR} have to be turned into another form, where the value of each scenario is in the same place as corresponding levels of occurrence. To achieve this transformation, again the decision variable b_{cap} is used to generate $b_{cap,re}$ a binary matrix with the dimension $B_{LAP} \times A_{mB}$, as shown in Equation 68. This matrix indicates the level of acceptance of each bid. Since each bid has a certain possibility of being not accepted, this must also be covered in the calculation. Therefore the flipped matrix $b_{cap,re,flip}$ is introduced in Equation 69. These two variables together with S_{PS} are used to create a matrix $b_{cap,mat}$ which allocate each scenario its corresponding place according to its level of occurrence S_{LoO}. Therefore the following Equations 70 and 71 are necessary.

$$b_{cap,re_{l,j}} = \sum_{i=1}^{T_{slot}} b_{cap_{j,1,l}}(i) \\ : \forall j \in \{1, ..., B_{LAP}\} \wedge \forall l \in \{2, ..., A_{mB}\} \tag{68}$$

$$b_{cap,re,flip_{l,j1}} = b_{cap,re_{l,j2}} \\ : \forall j1 \in \{1, ..., B_{LAP}\} \wedge j2 \in \{B_{LAP}, ..., 1\} \wedge \forall l \in \{2, ..., A_{mB}\} \tag{69}$$

$$b_{cap,mat_{j_1,...,j_{A_{mB}},m}} \leq b_{cap,re_{l,jj}} \cdot S_{PS_{l,m}} + aFRR_{cap,re,flip_{l,jj}} \cdot (1 - S_{PS_{l,m}} \\ : \forall jj \in \{j_1, ..., j_{A_{mB}}\} \wedge \forall \{j_1, ..., j_{A_{mB}}\} \in \{1, ..., B_{LAP}\} \wedge \\ \forall l \in \{1, ..., A_{mB}\} \wedge \forall m \in \{1, ..., PS\} \tag{70}$$

$$b_{cap,mat_{j_1,...,j_{A_{mB}},m}} \geq \left(\sum_{l=1}^{A_{mB}} b_{cap,re_{jj}}(l) \cdot S_{PS_m}(l) + b_{cap,re,flip_{jj}}(l) \cdot (1 - S_{PS_m}(l)) \right) - (A_{mB} - 1) \quad (71)$$
$$: \forall jj \in \{j_1, ..., j_{A_{mB}}\} \wedge \forall \{j_1, ..., j_{A_{mB}}\} \in \{1, ..., B_{LAP}\} \wedge$$
$$\forall m \in \{1, ..., PS\}$$

With the expected revenues of each scenario S_{EVR} and the binary variable $b_{cap,mat}$ allocating each scenario its corresponding place in matrix S_{LoO} describing the likelihood of occurrence of each scenario, these both can be combined to obtain one matrix $S_{EVR,cap,mat}$ with the expected revenues of each scenario S_{EVR} in its corresponding place in the likelihood of occurrence S_{LoO}. Since a multiplication of a variable and a binary variable are not possible in mixed integer linear programming a BIG-M formulation is used. As it is described in Equation 72 to 74.

$$S_{EVR,cap,mat} \geq 0 \quad (72)$$

$$S_{EVR,cap,mat_{j_1,...,j_{A_{mB}},m}} \leq S_{EVR_m}$$
$$: \forall \{j_1, ..., j_{A_{mB}}\} \in \{1, ..., B_{LAP}\} \wedge \quad (73)$$
$$\forall m \in \{1, ..., PS\}$$

$$S_{EVR,cap,mat_{j_1,...,j_{A_{mB}},m}} \geq M \cdot b_{cap,mat_{j_1,...,j_{A_{mB}},m}}$$
$$: \forall \{j_1, ..., j_{A_{mB}}\} \in \{1, ..., B_{LAP}\} \wedge \quad (74)$$
$$\forall m \in \{1, ..., PS\}$$

With $S_{EVR,cap,mat}$ describing the expected revenues of each scenario in its corresponding place and the likelihood of occurrence S_{LoO} matrix, the revenues value expected from the capacity tender for each scenario $r_{VE,cap,S}$ can be calculated as shown in Equation 75 buy adding all of the revenue values expected together $r_{VE,cap}$ the total revenue value expected from the capacity tender is calculated as it

is shown in Equation 76

$$r_{VE,cap,S_{j_1,...,j_{A_{mB}},m}} = S_{EVR,cap,mat_{j_1,...,j_{A_{mB}},m}} \cdot S_{LoO_{j_1,...,j_{A_{mB}}}} : \forall\{j_1,...,j_{A_{mB}}\} \in \{1,...,B_{LAP}\} \wedge \forall m \in \{1,...,PS\} \quad (75)$$

$$r_{VE,cap} = \sum_{i}^{PS} r_{VE,cap,S}(i) \quad (76)$$

To obtain the objective function of stage one the objective function shown in Equation 41 is extended with the total revenues expected from the positive and negative capacity tender.

$$obj_{S1} = obj_{IES} - R_{VE,cap,pos} - R_{VE,cap,neg} \quad (77)$$

3.5.2 MILP formulation - energy tender

In the following the formulation of the energy tender is described. It is implemented in stage two of the optimisation. This is necessary due to the fact, that it deals with parameters unknown in stage one. In stage two the real day ahead electricity prices are available. The bought and sold volume of electric energy, calculated in stage one, becomes a demand that has to be fulfilled. Placed bids in stage one are either accepted or declined, if they are accepted, the placed capacity must be offered in the corresponding time slot. In each different time-slot, it is possible to offer energy, but this not mandatory, since this fact, it is neglected in further considerations. Since the payment method is pay-as-cleared is used since summer of 2022 and the market is extreme volatile, a price prediction is not considered useful. The applied method is described in Section 3.3.

The formulation of stage two is mainly identical to the one the industrial energy system. As already mentioned results of stage one became parameters, as shown in Table 25 and demands which need to be full filled. Therefore the accepted bids are an input, as well as the called up power. If a bid from stage one is called up, the demand is adapted as shown in Equation 78. The formulation of the balancing energy is dropped in stage two, since it is no longer needed. Since the volume of the bought and sold electricity can no longer be changed P_{fG} and P_{tG} become parameters, and the costs and revenues of electricity are calculated according to Equation 79 and Equation 80. Since the structure is the same for both positive an

negative balancing energy, the indices to separate them are neglected. Equation 81 sows how the revenues of the balancing energy market for each bid and time slot are calculated, therefore as well the acceptance $A_{accepted}$ and the call up A_{callup} of the corresponding bid have to be one. The expected value of the revenue of the energy market is calculated in Subsection 3.3.4, and can be much higher but also lower. The power offered P_{offerd} is determined by stage one. The total expected revenues are calculated as seen in Equation 82. The objective function for stage two also changes, the expected revenues of the balancing energy have to be considered, which is shown in Equation 83.

Table 25: *Parameters and variables of stage two.*

Variable	Description	Unit	Dimension/Value
$P_{offerd,pos}$	Positive called up power	MW	$\mathbb{R}^{n\times 1}$
$P_{offerd,neg}$	Negative called up power	MW	$\mathbb{R}^{n\times 1}$
$c_{el,DA}$	Electricity costs per time step	€	$\mathbb{R}^{n\times 1}$
$r_{el,DA}$	Electricity revenues per time step	€	$\mathbb{R}^{n\times 1}$
$A_{accepted}$	Input about bid is accepted	-	$0, 1^{1\times A_{mB}}$
A_{callup}	Input about bid is called	-	$0, 1^{1\times A_{mB}}$
$A_{energy,rev}$	Expected value of the revenues of the energy market	€/MWh	$\mathbb{R}^{n\times 1}$
$r_{VE,energy,n}$	Expected revenues from the energy market for each time slot	€	$\mathbb{R}^{n\times A_{mB}}$
$r_{VE,energy}$	Expected revenues from the energy market	€	$\mathbb{R}$

$$P_{dem,elec,S2_i} = P_{dem,el_i} + P_{offerd,pos_i} - P_{offerd,neg_i} \quad : \forall i \in \{1, ..., n\} \tag{78}$$

$$c_{el,DA_i} = P_{fG_i} \cdot p_{real_i} \cdot \Delta T \quad : \forall i \in \{1, ..., n\} \tag{79}$$

$$r_{el,DA_i} = P_{tG_i} \cdot p_{real_i} \cdot \Delta T \quad : \forall i \in \{1, ..., n\} \tag{80}$$

$$r_{VE,energy,n_i} = A_{accepted_i} \cdot p_{real_i} \cdot A_{callup_i} \cdot P_{call} \cdot A_{energy,rev} \cdot \Delta T \quad : \forall i \in \{1, ..., A_{mB}\} \tag{81}$$

$$r_{VE,energy} = \sum_{i}^{A_{mB}} \sum_{j}^{n} r_{VE,energy,n}(i,j) \tag{82}$$

$$obj_{S2} = obj_{S1} - r_{VE,energy,pos} - r_{VE,energy,neg} \tag{83}$$

4 Results and Discussion

In this chapter, the results of the optimisation are presented and discussed. To quantify the benefits of participating in the balancing market, the optimization results are compared to several use cases. In Use Case 1, the balancing energy is not implemented and a constant electricity price is assumed. In Use Case 2 the electricity price prediction from the NARX neural network is used for the optimisation, and the total expanses are calculated with real prices, from the day-ahead auction. Use Case 1 and 2 are used for the purpose of verification. In Use Case 3A and Use Case 3B the balancing market is implemented, they represent the output of stage two. While at Use Case 3A no bid have been accepted or called, in Use Case 3B all bids are accepted and called. This chapter closes with the comparison of the four different use cases and an analysis of the obtained results.

4.1 Reference Use Cases

In this Section the two different reference models are explained in more detail. Therefore the main differences are highlighted. To be able to compare all these models the industrial energy system introduced in Section 3.4 stays the same for all of them.

4.1.1 Use Case 1 - constant electricity price

In Use Case 1, a constant electricity price is assumed, as it is the case for private consumers or middle sized companies. This constant electricity price is set to an average value for the real day-ahead price of the observed day with an surcharge of 20 % for buying and an reduction of 10 % when selling electrical energy.

4.1.2 Use Case 2 - DA-prediction

In Use Case 2, the price values for each hour, as predicted with the neural net described in 3.3.1, are used for the optimisation and expenses and revenues are

calculated with the real electricity price. The method of time depending electricity prices is used by energy intensive companies, but is also possible for private consumers.

4.2 Comparison

This section is separated, in three different subsection, the coverage of the electric and thermal demand, and the resulting expected revenues and costs. Each of these subsections explains the similarities and differences of the results between the four different use cases. Table 26 summarises all considers use cases and their main differences. The visual comparison in Subsection 4.2.1 and 4.2.2 is made for 30th of January and the resulting expected revenues and costs are calculated additional for 20th and 24th of January.

Table 26: *Description of the considered models.*

Name	Acronym	Description
Use Case 1	UC1	averaged real DA-price; surcharge for buy 20 %; reduction for sell 10 %
Use Case 2	UC2	optimisation with DA-prediction of the neural net; calculation of electricity cost with real price
Use Case 3A 1	UC3A	including aFRR; no bids are accepted or called
Use Case 3B 2	UC3B	including aFRR; all bids are accepted and called

4.2.1 Covering the electricity demand

This section shows how the electricity demand is met by the different use cases, as illustrated in Figure 21, Figure 22, Figure 23 and Figure 24. The x-axis shows the time steps in hours and the y-axis the produced electric power in MW. The power from the combined heat power plant is indicated with a blue bar. The electric energy, consumed by the boiler is in red. Solar energy is indicated by with the cyan bar. Electric energy form the DA electricity market is in yellow and the feed-in energy is indicated in purple. Energy stored or unsorted in or from the battery is visualised through green bars. The black curve is the electricity demand which need to be full filled. Since the electricity price is constant and more expensive the energy generated from the CHP, energy from the grid and the battery is used to meet energy peaks while the CHP covers the base load, shown in Figure 21. With the change from a constant to an flexible electricity price, the schedule changes

a lot. The CHP is no longer used to cover the base load over the whole day. In the morning and evening hours the predicted electricity price is cheaper than the produced energy from the CHP, shown in Figure 22. Due to the implementation of the aFRR capacity tender in Figure 23, the schedule again changes. To be able to ensure enough free positive and negative capacity, the CHP is switched on over the whole time period. In Figure 24 the electric demand changes compared to the Figures before, this is due to the accepted and called bids. Additionally the real electricity price is used here, but the amount of energy from or to the grid is no longer a variable. which leads again to a different schedule.

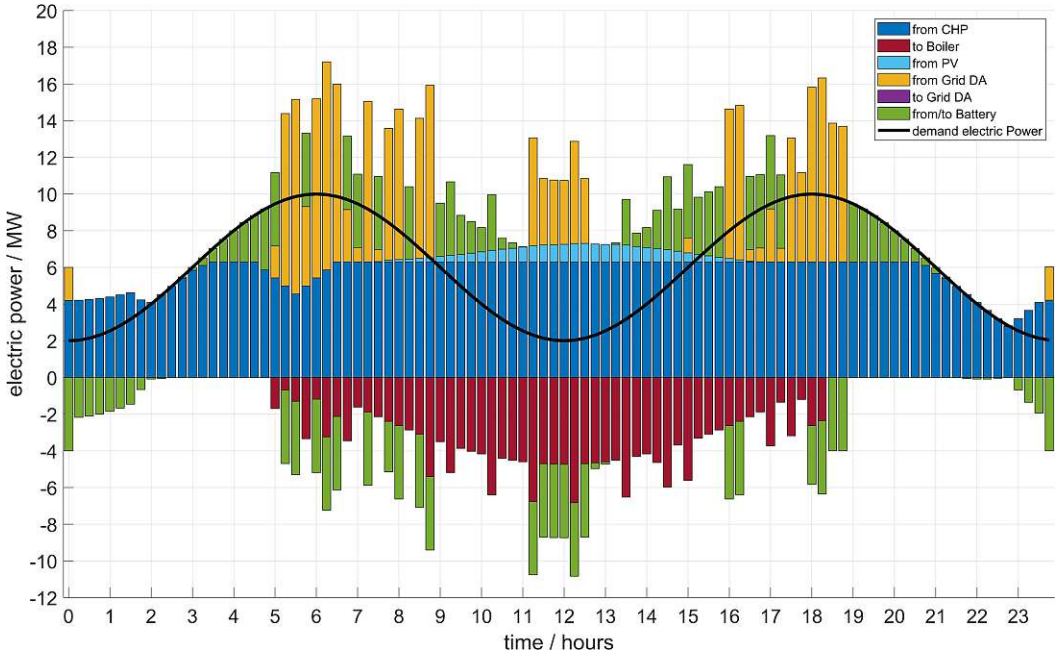

Figure 21: *Coverage of the electricity demand by UC1.*

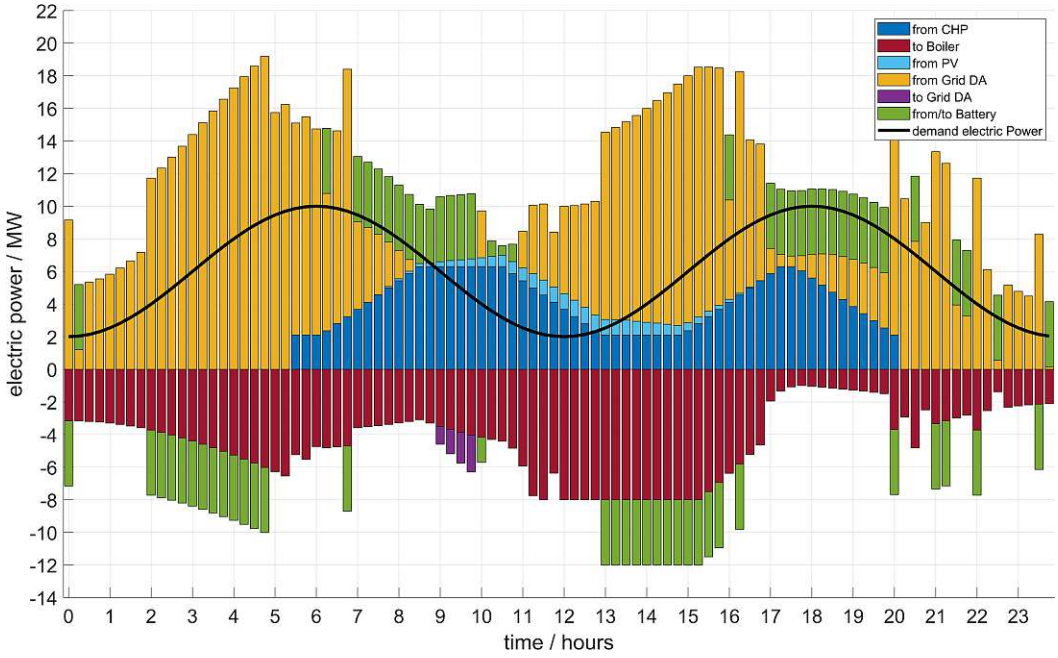

Figure 22: *Coverage of the electricity demand by UC2.*

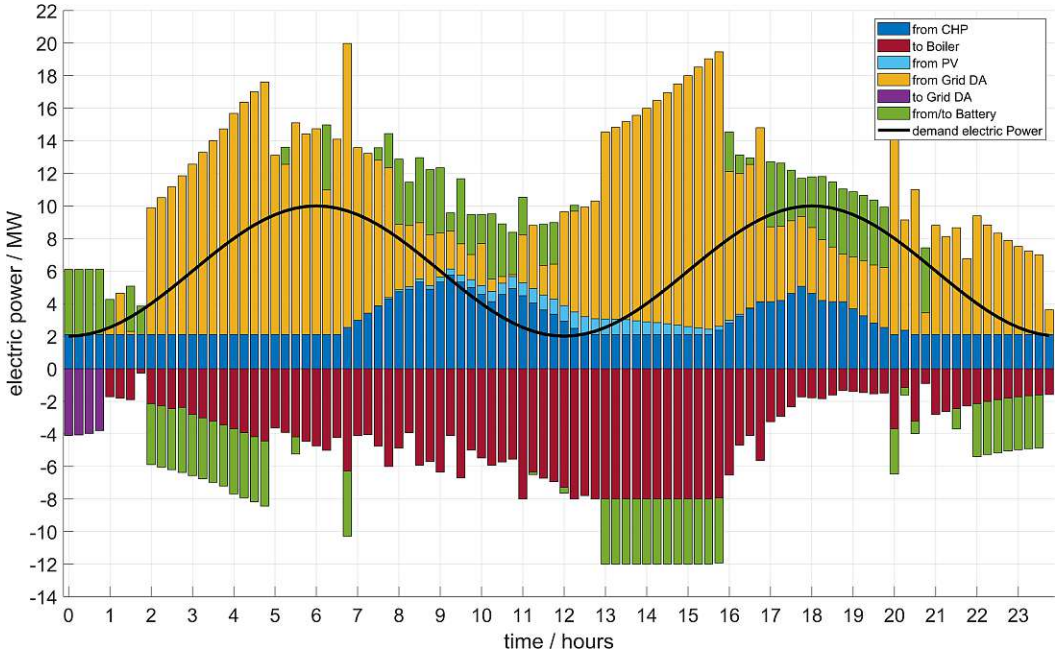

Figure 23: *Coverage of the electricity demand by UC3A.*

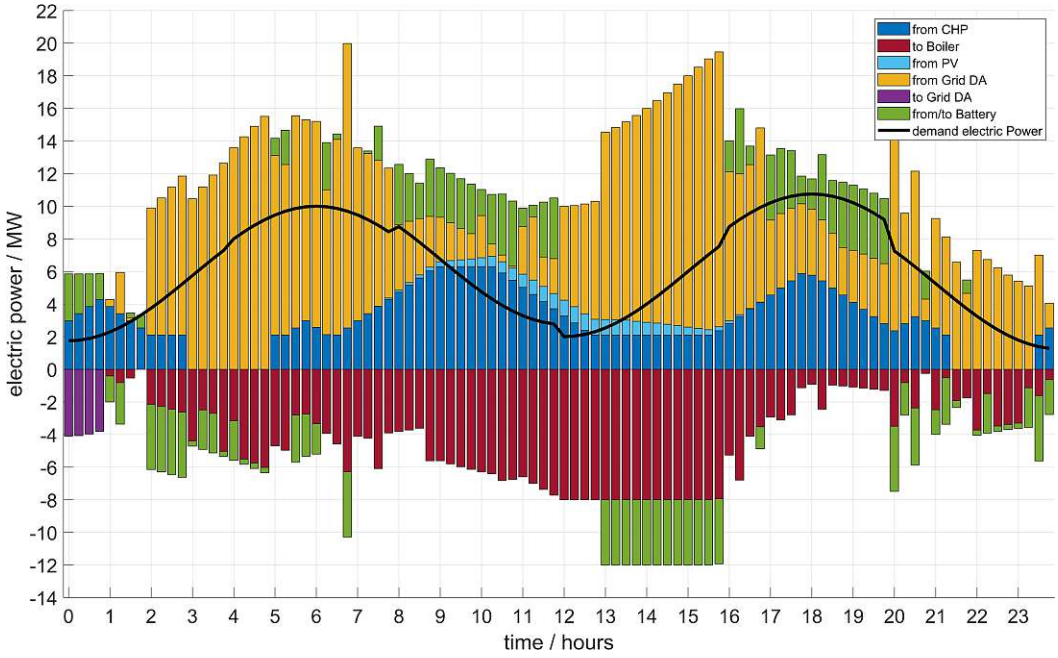

Figure 24: *Coverage of the electricity demand by UC3B.*

4.2.2 Covering the thermal demand

This section shows how the thermal demand is met by the different models, as illustrated in Figure 25, Figure 26, Figure 27 and Figure 28. The x-axis shows the time steps in hours and the y-axis the produced thermal power in MW. The power from the combined heat power plant is indicated with a blue bar. The thermal energy, produced by the boiler is shown in red. Waste heat is indicated trough purple bars. Energy stored or unsorted in or from the TES is visualised through orange bars. The black curve is the thermal demand which need to be full filed. The main differences in meeting the thermal demand result from the same reasons as in the electric demand.

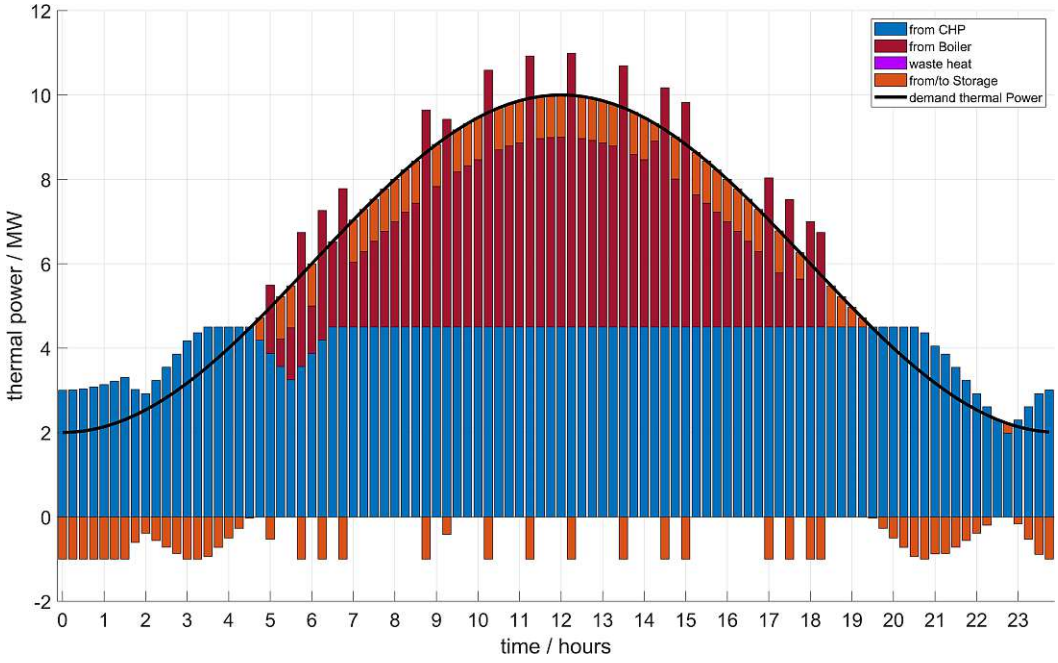

Figure 25: *Coverage of the thermal demand by UC1.*

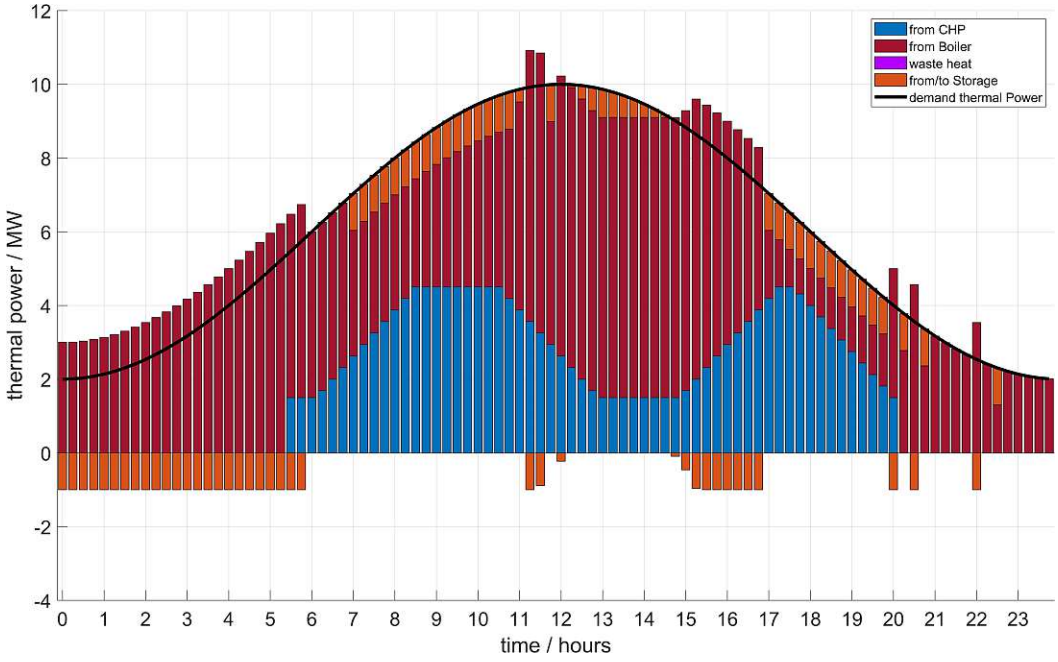

Figure 26: *Coverage of the thermal demand by UC2.*

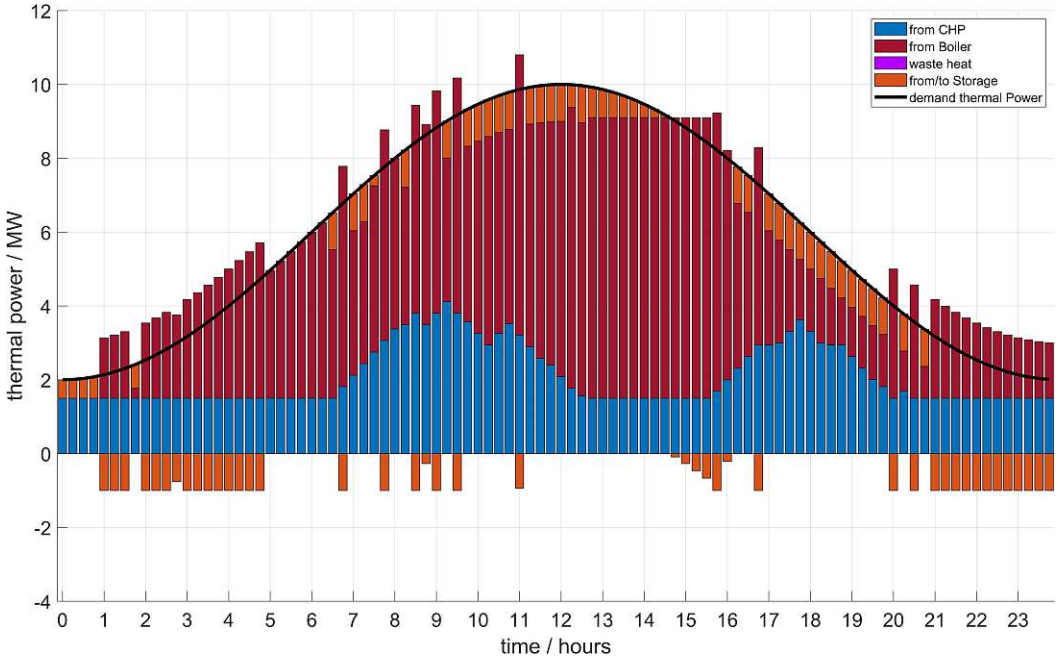

Figure 27: *Coverage of the thermal demand by UC3A.*

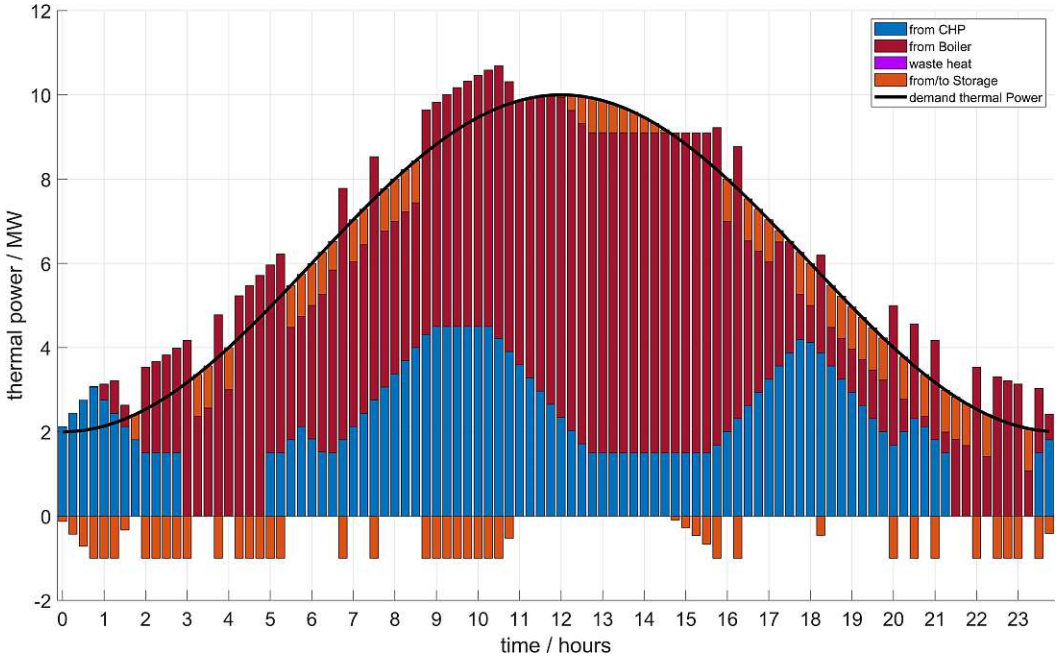

Figure 28: *Coverage of the thermal demand by UC3B.*

4.2.3 Revenues and costs

In this section the resulting expected revenues and costs of each of the models for all three considered days are compared, so it is possible to obtain the impact resulting form the implementation of the aFRR capacity tender. As seen in Table 27 there are big differences between the use cases. Use Case 1 is in every considered day the most expensive one, with an average value of 53 918 €. By using the day ahead prediction for the schedule of the industrial energy system and calculating the expenses with the real DA price, the costs are reduced to an average value of 50 000 €, which is a significant reduction. For USe Case 3A, where no bids are accepted or called, is not able to outperform Use Case 1, but it's expenses are lower than that one of Use Case 2, with a value of 51 768 €. In the case that all offered bids are accepted and called up, calculated with Use Case 3B, expenses are reduced to 45 456 €. This leads to the conclusion, that by implementing the aFRR into the given industrial energy system, the expenses can rise up to 3.5 % but can also be reduced by 9.1 % compared to the DA-predicted schedule, for the considered days. Additionally the

Table 27: *Overview and expected costs and revenues of January the all considered days.*

Costs/Revenues	UC1 €	UC2 €	UC3A €	UC3B €
20.01.2023	53 882	51 742	52 563	46 261
24.01.2023	55 300	51 284	54 003	47 701
30.01.2023	52 573	46 974	48 737	42 435
Average	53 918	50 000	51 768	45 456

expected costs and revenues are split according to their sources, to obtain more information about impact of the aFRR. This is shown in Table 28 for January the 20th in Table 29 for January the 24th and in Table 30 for January the 30th. For all of the considered three days the placement of the bids for the capacity tender are the same, which leads to the exact same revenues for each of the days. This result can be explained by the fact that monthly averages were used for PV output and the price level of the capacity market, and the demand for electricity and thermal energy is also independent of the day. Also worth noting is that the value for the reference model always lies between those results from optimisation models one and two.

Table 28: *Expected costs and revenues for January the 20th.*

Costs/Revenues	UC1 €	UC2 €	UC3A €	UC3B €
Fuel	43 129	6600	15 850	16 209
from Grid	10 753	45 142	37 407	37 407
to Grid	-	-	−694	−694
Capacity positive	-	-	-	−466
Capacity negative	-	-	-	−405
Energy positive	-	-	-	−5644
Energy negative	-	-	-	−145
Total	53 882	51 742	52 563	46 261

Table 29: *Expected costs and revenues for January the 24th.*

Costs/Revenues	UC1 €	UC2 €	UC3A €	UC3B €
Fuel	43 129	31 639	28 545	28 904
from Grid	12 171	21 147	26 114	26 114
to Grid	-	−1502	−656	−694
Capacity positive	-	-	-	−466
Capacity negative	-	-	-	−405
Energy positive	-	-	-	−5644
Energy negative	-	-	-	−145
Total	55 300	51 284	54 003	47 701

Table 30: *Expected costs and revenues for January the 30th.*

Costs/Revenues	UC1 €	UC2 €	UC3A €	UC3B €
Fuel	43 129	19 181	21 908	22 267
from Grid	9444	28 096	27 289	27 289
to Grid	-	−303	−461	−461
Capacity positive	-	-	-	−466
Capacity negative	-	-	-	−405
Energy positive	-	-	-	−5.644
Energy negative	-	-	-	−145
Total	52 573	46 974	48 737	42 435

5 Conclusion and Outlook

This last chapter starts with the presentation of the main findings during the work on this diploma thesis. The findings are evaluated and put into perspective. Finally, future investigation objectives and extensions to he developed optimisation model are suggested.

5.1 Conclusions

The nickname of the European energy system, the largest machinery built by mankind, is quite understandable. It takes a lot of effort to understand the different pillars and their needs. In detail, the balancing market itself is complex structure. As in the next Section 5.2 explained, the real world problem has to be reduced in its complexity, to be able to solve it in adequate time.
The choice of using a four dimensional decision variable for the implementation of aFRR capacity tender, is a very interesting attempt. On the positive side, with just two variables (positive and negative), the complete bidding behaviour of the optimisation is determined, which is indeed an advantage. But due the high dimensionality, calculations and constraint formulation become more complicated. Since mixed integer linear programming is used, multiplication of to variables is not possible. To be able to calculate the expected value of revenues for all different scenarios, a structure with non binary and binary variables has been implement. That lead to an increased calculation time, which strongly depends on the amount of bids.
The assumption, for historical averaged data of the capacity tender, may be not ideal, as the bid structure is the same for each considered day. For each of this days, it is possible to reduce the expenses, if the bids are called, if not, the expenses increase slightly.

5.2 Scope and limitations

In general, the implementation to be part automatic frequency restoration reserve tender is covered in this thesis. The FCR is neglected due to high requirements in prequalification. Manual frequency restoration reserve tender has similar requirements as aFRR, but is neglected since compensations are lower. In the optimisation the prequalifed level can be changed easily by changing on parameter, in real conditions this is much more difficult, since an approval procedure has to be done.
The input data are fraught with uncertainty. To obtain the level of acceptance probability, monthly averaged historical price data of the capacity tender are used, in the considered use cases the actual values of the corresponding months are used which does not describe the capacity tender ideal. It is a similar circumstance at the calculation of the energy tender. In the case of the forecast of the electricity price, a NARX neural net, is performed for every day, which is a much more accurate method.
The industrial energy system is subject to a number of simplifications. The coefficient of performance of the CHP and the boiler is constant over the whole working range. While the CHP has minimal power, the boiler can be operated continuous between zero and the maximum power. The thermal as well as the electric energy storage are ideal, meaning there are no losses by charging, discharging and storage in general. The photovoltaic system delivers the same averaged value for the corresponding month.
Due to the implementation of the capacity energy tender, the maximum charge and discharge rate of the electric storage is reduced, because of the assumption that only the battery is prequaified. In the case of the energy tender, electricity is either called up over the whole offered period or not, in real conditions everything in between is also possible.

5.3 Suggested future objectives

Since optimisation is based on input data, the quality of the results is strongly influenced by them. More accurate predictions and forecasts will therefore generally improve the optimisation. For this reason, regression analyses or neural networks could be used.

Another goal for the future is to convert the MATLAB® code used into a real-time system based on online data in order to obtain more accurate results. In the present MATLAB® code, the energy market is reduced to time slots in which a capacity is offered.

To obtain a more adequate model, the optimisation should be able to offer energy for each time slot. The implementation of the automatic frequency restoration reserve used here can be used as a first step for the implementation of the manual frequency restoration reserve.

Furthermore, a detailed consideration of the IES, especially with regard to the battery, leads to much more realistic results.

A test operation in which the results of the optimisation are compared with those of the tenders on the balancing energy market over a longer period of time would also be recommended.

Bibliography

[1] ENTSO-e. *Annual increase and decrease of net installed electricity generation capacity in Europe in 2022*. 2022. URL: https://energy-charts.info. (accessed: 01.03.2023).

[2] M. Ciucci. *Internal energy market*. 2022. URL: https://www.europarl.europa.eu/factsheets/en/sheet/45/internal-energy-market. (accessed: 01.03.2023).

[3] EU-Council. *REPowerEU: Council agrees on accelerated permitting rules for renewables*. 2022. URL: https://www.consilium.europa.eu/en/press/press-releases/2022/12/19/repowereu-council-agrees-on-accelerated-permitting-rules-for-renewables/. (accessed: 01.03.2023).

[4] Enspired-trading. *Uniform pricing*. 2022. URL: https://www.enspired-trading.com/blog/uniform-pricing. (accessed: 20.03.2023).

[5] ENTSO-e. *Single Day-ahead Coupling (SDAC)*. 2022. URL: https://www.entsoe.eu/network_codes/cacm/implementation/sdac/. (accessed: 01.03.2023).

[6] ENTSO-e. *Single Intraday Coupling (SIDC)*. 2022. URL: https://www.entsoe.eu/network_codes/cacm/implementation/sidc/. (accessed: 01.03.2023).

[7] APG. *NETZFREQUENZ*. 2022. URL: https://markttransparenz.apg.at/de/markt/Markttransparenz/Netzregelung/Netzfrequenz. (accessed: 01.03.2023).

[8] APG. *Netzregelung*. 2022. URL: https://markt.apg.at/netz/netzregelung/. (accessed: 01.03.2023).

[9] APG. *Primärregelung (PRR)*. 2022. URL: https://markt.apg.at/netz/netzregelung/primaerregelung/. (accessed: 01.03.2023).

[10] APG. *Sekundärregelung (SRR)*. 2022. URL: https://markt.apg.at/netz/netzregelung/sekundaerregelung/. (accessed: 01.03.2023).

[11] ENTSO-e. *Platform for the International Coordination of Automated Frequency Restoration and Stable System Operation (PICASSO)*. 2022. URL: https://www.entsoe.eu/network_codes/eb/picasso/. (accessed: 01.03.2023).

[12] APG. *Austrian Power Grid: So helfen PICASSO und MARI Stromkosten zu senken und Erneuerbare zu integrieren*. 2020. URL: https://markt.apg.at/news/austrian-power-grid-so-helfen-picasso-und-mari-stromkosten-zu-senken-und-erneuerbare-zu-integrieren/. (accessed: 01.03.2023).

[13] APG. *Tertiärregelung (TRR)*. 2022. URL: https://markt.apg.at/netz/netzregelung/tertiaerregelung/. (accessed: 01.03.2023).

[14] ENTSO-e. *Manually Activated Reserves Initiative (MARI)*. 2022. URL: https://www.entsoe.eu/network_codes/eb/mari/. (accessed: 01.03.2023).

[15] K. S. Deepak Singhal. "Electricity price forecasting using artificial neural networks". In: *Electrical Power and Energy Systems* 33 (2006), pp. 550–555. ISSN: 01420615.